Identifying landscape hot and cold spots of soil GHG fluxes by combining field measurements and remote sensing data

Authors: Elizabeth Gachibu Wangari[1], Ricky Mwangada Mwanake[1], Tobias Houska[2], David Kraus[1], Gretchen Maria Gettel[3,4], Ralf Kiese[1], Lutz Breuer[2,5], Klaus Butterbach-Bahl[1,6]

[1]Karlsruhe Institute of Technology, Institute for Meteorology and Climate Research, Atmospheric Environmental Research (IMK-IFU), Kreuzeckbahnstrasse 19, Garmisch-Partenkirchen 82467, Germany

[2]Institute for Landscape Ecology and Resources Management (ILR), Research Centre for BioSystems, Land Use and Nutrition (iFZ), Justus Liebig University Gießen, 35392 Gießen, Germany

[3]IHE Delft Institute for Water Education, Westvest 7, 2611 AX Delft, The Netherlands.

[4]Department of Ecoscience, Lake Ecology, University of Aarhus, Aarhus Denmark

[5]Centre for International Development and Environmental Research (ZEU), Justus Liebig University Giessen, Senckenbergstrasse 3, 35390 Giessen, Germany

[6]Pioneer Center Land-CRAFT, Department of Agroecology, University of Aarhus, C. F. Møllers Allé 4, Building 1120, Aarhus 8000, Denmark

Correspondence to: Klaus Butterbach-Bahl (klaus.butterbach-bahl@agro.au.dk)

Keywords: Soil respiration, Ecosystem respiration, Methane uptake, Nitrous oxide fluxes, Random forest algorithm, upscaling, Arable, Grassland, Forest

Abstract

Upscaling chamber measurements of soil greenhouse gas (GHG) fluxes from points to landscape scales remain challenging due to high variability of fluxes in space and time. This study measured GHG fluxes and soil parameters at selected point locations (n=268), thereby implementing a stratified sampling approach on a mixed land-use landscape (~5.8 km^2). Based on these field-based measurements and remotely-sensed data on landscape and vegetation properties, we used Random Forest models to predict GHG fluxes at a landscape scale (1 m resolution) in summer and autumn. The results showed improved GHG flux prediction performance when combining field-measured soil parameters with remotely-sensed data. Available satellite data products from Sentinel-2 on vegetation cover and water content played a more significant role than attributes derived from a digital elevation model, possibly due to their ability to capture both spatial and seasonal changes of ecosystem parameters within the landscape. Similar seasonal patterns of higher soil/ecosystem respiration (SR/ER-CO$_2$) and nitrous oxide (N$_2$O) fluxes in summer and higher methane (CH$_4$) uptake in autumn were observed in both the measured and predicted landscape fluxes. Based on the upscaled fluxes, we also assessed the contribution of hot spots to total landscape fluxes. The identified emission hot spots occupied a small landscape area (7 to 16%) but accounted for up to 42% of the landscape GHG fluxes. Our study showed that combining remotely-sensed data with chamber measurements and soil properties is a promising approach for identifying spatial patterns and hot spots of GHG fluxes across heterogeneous landscapes. Such information may be used to inform targeted mitigation strategies at landscape-scale.

1. Introduction

Atmospheric concentrations of greenhouse gases (GHGs) such as carbon dioxide (CO_2), methane (CH_4), and nitrous oxide (N_2O) have increased since the 1750s, substantially driving global climate change (IPCC, 2019). Soils are key contributors to these GHG fluxes, with recent global emissions of approximately 350 Pg CO_2 equivalents per year (Oertel et al., 2016). Soil GHG emissions have accelerated due to human activities such as land use change for agricultural land expansion (Dhakal et al., 2022). Globally, agricultural soils are significant sources accounting for about 37% of the GHG emissions within the agricultural sector (Tubiello et al., 2013). However, the estimates of soil GHG fluxes are highly uncertain since soil properties, land use, and land management, which are key indirect drivers of the emissions, largely differ across landscapes and regions. For instance, global annual estimates range widely from 67 to 101 Pg C (Jian et al., 2018) for soil respiration, 2.5 – 6.5 Tg N_2O-N for annual soil N_2O emissions (Tian et al., 2020), and 12 – 60 Tg for soil CH_4 uptake rates (Dutaur & Verchot, 2007). These uncertainties make it difficult to accurately quantify the GHG source or sink strengths of soils and to develop targeted mitigation options across scales.

Current upscaling approaches from localized measurements of soil GHG fluxes to landscape or regional scales using chamber or site-specific micro-meteorological methods such as eddy-covariance (e.g., Sundqvist et al., 2015; Vainio et al., 2021, Warner et al., 2018; Han et al., 2022), fail to capture the spatio-temporal variation of hot- or cold-spots, resulting in uncertainties in regional and global GHG estimates (Hagedorn & Bellamy, 2011; Levy et al., 2022). Contrary to the eddy-covariance method, chamber-based approaches can be used to capture fine-scale spatial variabilities of soil GHG fluxes within landscapes, e.g., when measurements are conducted at sampling sites representative of the spatial heterogeneities related to land use, land management, and topography (e.g., Warner et al., 2018; Vainio et al., 2021; Wangari et al., 2022). However, the ability of chambers to accurately quantify landscape fluxes over relatively larger areas is limited and closely related to the number of chamber measurement locations per unit area (Wangari et al., 2022). Previous studies have shown that the uncertainties in landscape-scale fluxes from chamber measurements using area-weighted averages increase exponentially with a decrease in the number of chamber measurement locations (e.g., Arias-Navarro et al., 2017; Wangari et al., 2022). Nevertheless, the practicability of increasing the number of chamber measurement locations to quantify landscape fluxes is constrained by extensive human and technical resource requirements, hence there is a need for alternative ways of estimating GHG landscape fluxes.

The limitation of extensive chamber measurements required to quantify landscape fluxes can be overcome through modeling approaches that offer cost-effective and more practical alternatives. Machine learning (ML) algorithms are increasingly used to gap-fill spatio-temporal datasets on soil GHG fluxes as they require lesser computational time and expertise than complex biophysical models (Dorich et al., 2020; Zhang et al., 2020; Saha et al., 2021; Adjuik & Davis, 2022; Joshi et al., 2022). Amongst the available ML algorithms, the random forest (RF) algorithm has been evaluated as one of the best for predicting soil GHG fluxes (Hamrani et al., 2020; Adjuik &

69   Davis, 2021; Han et al., 2022). The RF algorithm has been widely applied to gap-fill and upscale soil GHG fluxes in

70   temperate ecosystems from point measurements to larger scales, with relatively better prediction accuracies (e.g.,

71   Philibert et al., 2013; Räsänen et al., 2021; Vainio et al., 2021).

72   Several studies have explored the use of high-resolution remote-sensing (RS) datasets such as digital

73   elevation models (DEMs) and indices from spectral characteristics derived from satellite images in combination with

74   on-site chamber measurements to predict landscape GHG fluxes (e.g., Sundqvist et al., 2015; Warner et al., 2018;

75   Vainio et al., 2021; Räsänen et al., 2021). These studies used RS datasets on landscape and vegetation parameters as

76   proxies for soil physical and chemical characteristics such as soil moisture, soil vegetation cover, and nutrient

77   availability, i.e., key biogeochemical drivers of soil GHG fluxes. However, the above studies have either been

78   conducted over relatively small areas or have focused on individual land uses and GHG fluxes. For instance, only

79   one study has applied a RF approach to predict CH_4 fluxes for a larger (12.4 km^2) peatland-forested landscape based

80   on RS data and 279 on-site measurements of soil temperature, moisture, and vegetation (Räsänen et al., 2021). In

81   addition, spatial CO_2 and CH_4 fluxes have been predicted for relatively small (~0.1 km^2) forested landscapes using

82   DEM-derived terrain attributes and a few site-measured (temperature and moisture) soil variables (Warner et al.,

83   2018; Vainio et al., 2021). Applying RF models using various RS datasets and soil parameters for soil GHG flux

84   predictions on larger and heterogeneous landscapes in relation to land use, topography, and soil conditions remains

85   unexplored. It is still uncertain whether such landscape flux predictions would improve if supplemented by multiple

86   actual field measurements of soil properties (e.g., texture) and variables (e.g., inorganic N content), which may better

87   describe the geochemical and physical conditions compared to RS-derived indices.

88   In this study, we aimed to determine the potential of applying the RF algorithm to predict the spatial and

89   seasonal variability of soil CO_2, CH_4, and N_2O fluxes using a high number of stratified sampling locations (n = 268)

90   spread across a relatively large (~5.8 km^2) landscape with heterogeneous land uses (forest, grassland, and arable

91   land). Specifically, we aimed to: (a) evaluate the effectiveness of high-resolution RS data and relatively low-

92   resolution data on soil physico-chemical parameters in predicting soil GHG fluxes across different land uses; (b)

93   predict high-resolution soil GHG fluxes at a landscape scale and detect GHG hot spots and cold spots; and (c)

94   compare landscape GHG fluxes upscaled from RF-predicted high-resolution maps with aggregated landscape flux

95   estimates from averaged (point) fluxes multiplied by landscape area. We hypothesized improved prediction

96   accuracies using a combination of RS datasets that act as proxies of key drivers of soil GHG fluxes (e.g., vegetation

97   cover and water content) and the site-measured soil parameters representing the actual field conditions. We expected

98   fine-scale hot spots (within a few meters) to occur in cultivated areas and cold spots in forested areas. We also

99   hypothesized that the high-resolution upscaled fluxes from the RF approach, which better captures hot and cold spot

100   regions across the landscape, would avoid possible under- or overestimations of landscape fluxes derived from land

101   use specific area-weighted averages calculated from few point chamber measurement locations.

2. Materials and methods

2.1 Study area

The study area is located within the Schwingbach catchment in Hesse, central Germany (50°30'4.23. N, 8°33'2.82. E). The landscape covers an area of approximately 5.8 km^2, excluding the human settlement areas and road networks. Land uses within the landscape are mainly forests (57%) and arable lands (34%). Grasslands cover about 8% and are primarily located in riparian zones (Figure 1). The dominant soil types are cambisol (69%, forest and arable), stagnosol (23%, mainly arable), and gleysol (5%) which are found along grassland riparian zones (Wangari et al., 2022). The topsoils (0 – 5 cm) in the arable and grasslands have a silt loam texture, while the topsoils in the forest land mostly have a sandy loam texture (Sahraei et al., 2020). The landscape has an average slope of 5% with an elevation range of 233 – 415 m a.s.l. The region has a temperate oceanic climate (Cfb, Köppen climate classification) with annual average precipitation and temperature of 623 mm and 9.6°C based on long-term data (1969 – 2019) (Sahraei et al., 2021).
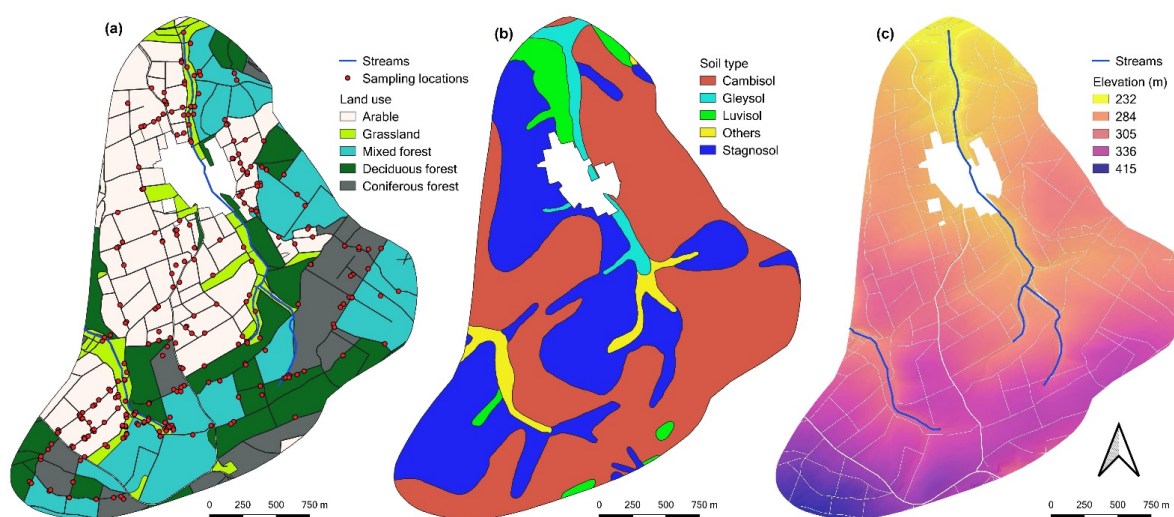
Figure 1: Map showing (a) the land uses and the location of the stratified sampling sites (selected based on combined classes of land use, slope, and soil type) across the study area; (b) the soil types; and (c) the digital elevation model (DEM; 1 m resolution) of the landscape (source of DEM: Hessische Verwaltung für Bodenmanagement und Geoinformation, https://hvbg.hessen.de/).

2.2 Soil physico-chemical parameters and GHG fluxes

2.2.1 Point measurements

Soil sampling and GHG flux measurements (CH_4, N_2O, and CO_2) were conducted at spatially distributed sampling sites across the study landscape (see Tab. 1 for a list of observed variables). We used a stratified random sampling approach to distribute 270 sites across different land uses (forest, grassland, and arable), soil types (cambisol, stagnosol/gleysol, and luvisol), and slopes (0–5, 6–11, and >11%) to capture the spatial variability of soil GHG fluxes and the driving parameters (Wangari et al., 2022). Out of the 270 targeted locations, field measurements were conducted at 246 sites in the summer (30th June – 9th July, field measuring campaign 1) and 268 sites in the autumn (8th – 17th September, field measuring campaign 2) of 2020. The estimated number of measured points for the forest, grassland, and arable ecosystems was ~25, 150, and 28 per km^2 (Table 1). We allocated more grassland sites due to the hypothesis that riparian grasslands are hot spots of GHG fluxes.

Soil GHG flux measurements were performed during the day (7.00 am – 5.00 pm) using a fast-box chamber technique (Hensen et al., 2013; Butterbach-Bahl et al., 2020). The CO_2 concentrations in the opaque chamber headspace were measured with an infrared gas analyzer (LI-840A & LI-850, LI-COR Biosciences, Lincoln, NE, USA), while CH_4 and N_2O concentrations were measured with an Off-Axis Integrated Cavity Output Spectroscopy (OA-ICOS) analyzer (Los Gatos Research, Inc., CA, USA). The GHG fluxes were calculated based on the linear changes of gas concentrations in the chamber headspace in the first 5-7 minutes following chamber closure. The soil sampling, analysis, and flux measurement methods are detailed in Wangari et al. (2022).

Table 1: List of the soil physico-chemical parameters and remotely-sensed data used in this study to upscale the GHG fluxes and details of the spatial resolutions of the maps.

Category	Predictor variables	Resolution		Source
		Original	Final	
	Elevation	1 m	1 m	Hessische Verwaltung für Bodenmanagement und
Remotely-sensed data (RS)	Slope	1 m	1 m	
	Aspect	1 m	1 m	Calculated from elevation
	Topographic wetness index (TWI)	1 m	1 m	
	Topographic position index (TPI)	1 m	1 m	
	Normalized difference vegetation index (NDVI)	10 m	1 m	Copernicus Sentinel-2 (European Space Agency)
	Green normalized difference vegetation index (GNDVI)	10 m	1 m	
	Normalized difference moisture index (NDMI)	20 m	1 m	
Soil physico-chemical parameters (SP)	Soil temperature (°C)		1 m	
	Gravimetric soil moisture (%)		1 m	
	pH		1 m	
	Bulk density (g cm^{-3})		1 m	
	NO$_3$-N (mg kg^{-1} dry soil)	~ 25, 150, and 28 sites per km^2 in forest, grassland, and arable land	1 m	Interpolated from sampling point data measured in summer and autumn (Wangari et al. 2022)
	NH$_4$-N (mg kg^{-1} dry soil)		1 m	
	DOC (mg kg^{-1} dry soil)		1 m	
	TDN (mg kg^{-1} dry soil)		1 m	
	Soil TN (%)		1 m	
	Soil TOC (%)		1 m	
	CN		1 m	
	Sand content (%)		1 m	
	Silt content (%)		1 m	
	Clay content (%)		1 m	

2.2.2 Spatial interpolation of soil parameters

Upscaling soil GHG fluxes using the RF algorithm required spatial raster maps of the soil physico-chemical predictor parameters. Thus, we interpolated our measured point data to continuous landscape maps using the inverse distance weighted (IDW) approach in the System for Automated Geoscientific Analyses software (SAGA: QGIS) with a distance coefficient power of 1 (Gradka & Kwinta 2018). The spatial interpolations were performed per land use (forest, grassland, and arable land) and for each season (summer and autumn) due to significant variations in soil parameters such as soil moisture or inorganic N content across land uses and seasons (see Wangari et al., 2022).

2.3 Remote sensing data

We retrieved several landscape-scale remote-sensing images with spatial data representing potential drivers of soil GHG fluxes, such as vegetation cover and vegetation water content. Landscape elevation was acquired from a high-resolution (1 m) digital elevation model (DEM) retrieved from the Hessische Verwaltung für Bodenmanagement und Geoinformation on March 1, 2022 (link source). Slope and aspect were calculated from the

151 DEM using the "r.slope.aspect" function in QGIS. We further computed the topographic position index (TPI) and

152 topographic wetness index (TWI) from the DEM using the terrain analysis plugin in QGIS. Vegetation information

153 on chlorophyll and water content was derived from satellite bands of Sentinel-2 images. Satellite images with low

154 (<1%) cloud cover were accessed from the ESA Copernicus Open Access Hub (link source; accessed on March

155 2021) using the Semi-Automatic Classification Plugin (SCP) in QGIS for each field measuring period. The

156 normalized difference vegetation index (NDVI) and the green normalized difference vegetation index (GNDVI) were

157 calculated using the near-infrared (NIR), red, and green bands (Bannari et al. 1995; Gitelson and Merzlyak, 1998;

158 Eq. 1 and 2). Compared to NDVI, GNDVI has a higher ability to detect differences in the chlorophyll content of

159 plants, especially later in the vegetation period, due to the higher chlorophyll sensitivity of the green band in GNDVI

160 than the red band in NDVI. The vegetation water content was estimated using the normalized difference moisture

161 index (NDMI), which was computed using the NIR and short-wave infrared (SWIR) bands (Gao, 1996; Malakhov

162 and Tsychuyeva, 2020; Eq. 3). We uniformly downscaled the resolutions of these remotely-sensed vegetation indices

163 to match the 1 m spatial resolution of the DEM-derived data files (Table 1).

164 $$NDVI = \frac{NIR-RED}{NIR+RED} \qquad \text{(Eq. 1)}$$

165 $$GNDVI = \frac{NIR-GREEN}{NIR+GREEN} \qquad \text{(Eq. 2)}$$

166 $$NDMI = \frac{NIR-SWIR}{NIR+SWIR} \qquad \text{(Eq. 3)}$$

167 **2.4 Random Forest regression model**

168 RF model development and prediction of the GHG fluxes were performed per land use (forest, grassland,

169 and arable) because there were statistically significant differences observed in the measured fluxes and the

170 underlying GHG flux controls of soil parameters for the different land uses (Wangari et al., 2022). For instance, N_2O

171 fluxes and soil nitrate concentrations were up to two-fold higher in arable soils than in forestry or grassland soils.

172 The CH_4 uptake rates of grassland and arable soils were lower than those of forest soils due to general differences in

173 soil structure, nitrogen concentrations, and disturbances (Wangari et al., 2022). We trained models using merged

174 summer and autumn point data to enable larger and temporally representative datasets for training models that could

175 estimate low and high landscape GHG fluxes (Figure 2).

176
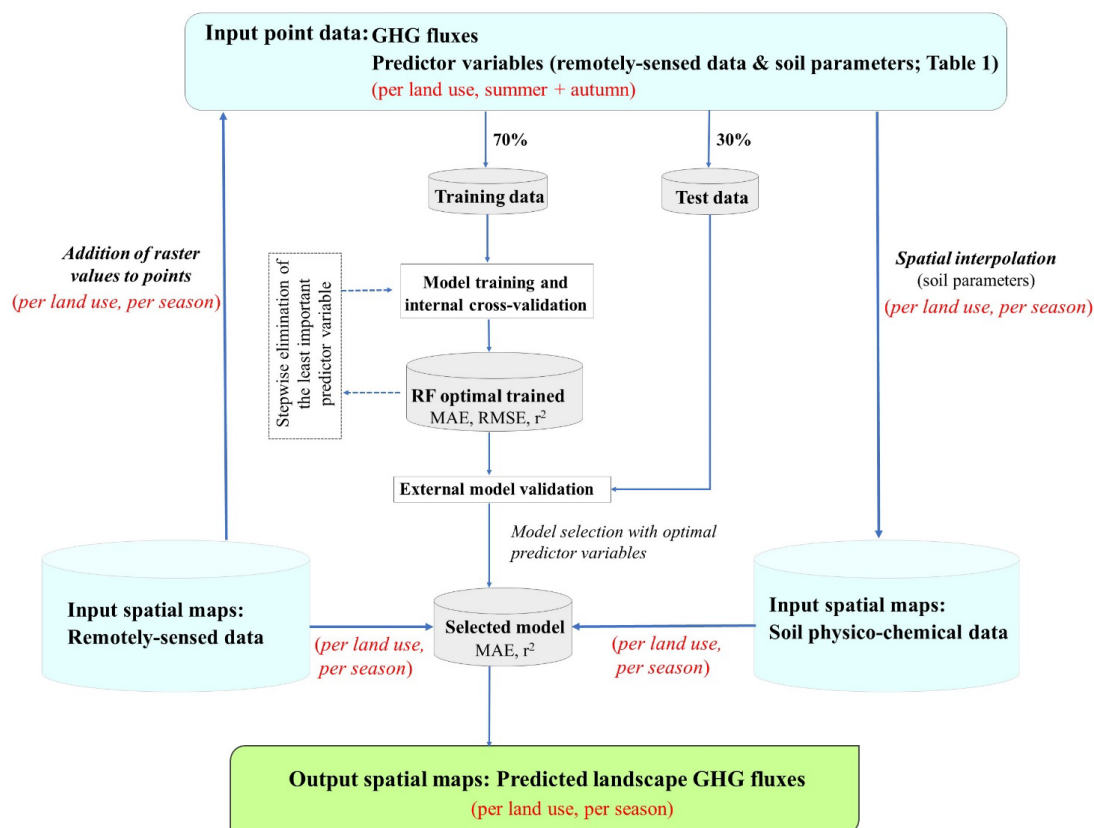
Figure 2: Workflow summary showing the input data (in blue), the approach used for RF model development and prediction of landscape fluxes, and the performance evaluation metrics (MAE, RMSE, and r^2).

We used the RF algorithm built in the CARET (classification and regression training) package in R to predict the soil GHG fluxes at a landscape scale (Breiman, 2001; Kuhn, 2008). For model development, the input datasets were split into a training and internal cross-validation set (70%) and an external test set (30%) using a stratified random sampling method. We defined a ten-fold (K=10) repeated cross-validation scheme using the 'trainControl' function to internally validate our trained models and prevent model overfitting (Berrar, 2018). A seed value of 123 was specified using the 'set.seed' function to enable reproducible results each time we ran a specific model. The optimal trained model was automatically selected using the mean absolute error (MAE) metric with the least value. The predictor variables in the optimal trained model were then ranked according to their importance using the RF variable importance measure in the 'varImp' function. Subsequently, stepwise elimination of the least essential variable was performed to quantify the predictive power of landscape GHG fluxes using fewer predictor variables (Figure 2).

To assess the effectiveness of various types of predictors in modeling landscape fluxes, we defined three categories of datasets, namely remote-sensing (RS), site-measured soil physico-chemical parameters (SP), and combined data (CD) (Table 1). Several RF models were trained following the stepwise elimination of the least

193 important variables in each data category (RS, SP, CD). Since 88% of CH$_4$ fluxes were negative and 86% of N$_2$O

194 fluxes were positive (Wangari et al., 2022), we additionally trained models using only the negative CH$_4$ and positive

195 N$_2$O flux datasets to compare their performances with the models built with all (positive and negative) fluxes.

2.5 Model performance assessment and prediction of landscape fluxes

197  The performance assessment metrics of the trained models included MAE, root mean square error (RMSE),

198 and the coefficient of determination (r^2) from the internal cross-validation. The final models for predicting landscape

199 fluxes in each data category (RS, SP, CD) were selected based on the highest possible r^2 with a relatively low MAE.

200 For each season and land use, the surface maps of the respective predictor variables in the final models were merged

201 using the raster brick function in R. The spatial fluxes for each land use were then predicted based on the selected

202 model and the input raster brick using the 'predict' function in R. To improve the prediction performance, the non-

203 normal distributed (SR/ER_CO$_2$ and N$_2$O) fluxes were log-transformed before model development. After prediction,

204 the transformed fluxes were retransformed using an exponential function.

205  Further evaluation of the model performances was conducted through linear regression and correlation

206 analysis of observed against retransformed predicted fluxes for all sampling sites. An additional external validation

207 step was performed using the measured and predicted fluxes of the sampling sites in the 30% test dataset that was

208 excluded from the model development. For this analysis, we compared the predicted mean fluxes (using RS, SP, and

209 CD datasets) with the observed mean fluxes. Analyses of variances (Type II) from linear mixed-effects models

210 ("nlme" package in R) were used to compare these arithmetic means. The fixed effects in the mixed models were

211 seasons (summer and autumn) and GHG flux type (measured and predicted fluxes from the RS, SP, and CD

212 datasets). Random effects of site variability were also included in the mixed models. The measured and predicted

213 fluxes were log-transformed to the normality assumption. A Tukey post-hoc test (p-value <0.05) of least square

214 means was used on the mixed models to identify statistically significant differences between the measured, RS-

215 predicted, SP-predicted, and CD-predicted fluxes.

216  Since many traditional GHG upscaling approaches rely on aggregated fluxes (area-weighted averages), we

217 also estimated spatial fluxes for the summer and autumn seasons using this technique. GHG fluxes were aggregated

218 on the landscape scale by multiplying the average fluxes measured for each land use by the area of each land use. We

219 compared the total landscape fluxes upscaled using this conventional aggregation technique of average fluxes with

220 the spatial fluxes predicted using the modeling approach.

2.6 Identification of GHG 'hot' and 'cold' spots from predicted landscape fluxes

222  Statistical approaches were deployed to identify areas that may have disproportionately contributed to the

223 overall landscape GHG fluxes (e.g., van Kessel et al., 1993; Mason et al., 2017). We defined the threshold for hot

224 spots using the sum of the median (M) flux and the interquartile (Q3-Q1) flux range (Eq. 4). Thus, the hot spots

225 within the landscape were identified as the areas with flux values greater (lower for CH$_4$ uptake) than the set hot spot

226 threshold. We fixed an inverse threshold (Eq. 5) for cold spots and identified cold spot patches with fluxes below

227 (above for CH$_4$ uptake) this threshold. Common emission hot spots were defined as the areas with overlapping

228   elevated emissions of the three GHG fluxes (SR/ER-CO_2, CH_4, and N_2O) within the landscape. The average

229   (summer and autumn) landscape fluxes were used to identify the hot and cold spots. We also calculated season-

230   specific thresholds to compare the increase and decrease of hot and cold spot areas between summer and autumn.

231         $Hot\ spot\ threshold = M + (Q3 - Q1)$ (Eq. 4)

232         $Cold\ spot\ threshold = M - (Q3 - Q1)$ (Eq. 5)

3. Results

3.1 RF model performance

The performance of the final models selected for the prediction of landscape fluxes varied across input datasets (RS, SP, and CD), GHG fluxes (SR/ER_CO$_2$, CH$_4$, and N$_2$O), and land use (forest, grassland, and arable land) (Table 2). The predictive performance (r^2) from the internal cross-validation step was higher in the models using the CD dataset (range: 0.15 – 0.78) than those using the RS (range: 0.13 – 0.73) and SP (range: 0.15 – 0.63) datasets (Table 2). The RF models predicting SR/ER_CO$_2$ fluxes had much higher r^2 (range: 0.45 – 0.78) than those predicting N$_2$O and CH$_4$ fluxes (range: 0.13 – 0.56). Arable ecosystem models resulted in much better predictions of SR/ER_CO$_2$ (r^2 range: 0.63 – 0.78) and N$_2$O (r^2 range: 0.45 – 0.56) fluxes compared to those for forest and grassland ecosystems across all data categories (Table 2). The prediction of CH$_4$ fluxes was also better for arable lands, but only when using the RS data (Table 2). Stepwise elimination of the least important variables had a minimal effect on the performances of the trained models (Table B1-B5 in Appendices). The selected models for the different categories of datasets (RS, SP, and CD) had varying predictor variables across land uses. The forest and grassland models required the most (5 and 6) predictor variables. In contrast, the least number of predictors (2) were mainly observed for models describing GHG fluxes from arable soils, especially in the RS and SP categories (Table 2).

Comparing the models (CD) applied to predict the landscape fluxes, the site-measured soil moisture content was a key predictor variable for all three GHG fluxes across land uses. In addition to soil moisture, the measured soil nitrogen content (NH$_4$ or SN) and remotely sensed vegetation indices (NDVI, GNDVI, or NDMI) were prevalent predictors of landscape SR/ER_CO$_2$ fluxes. Soil nitrogen content (NO$_3$ or CN) was also a recurrent predictor of CH$_4$ fluxes across land uses. However, the landscape CH$_4$ models had other varying predictors, such as aspect and soil temperature in forest models, pH and clay in grassland, and vegetation indices in arable ecosystem models. For N$_2$O, soil inorganic nitrogen (NH$_4$ or NO$_3$) concentrations predicted the fluxes in the forested areas, while vegetation indices were common predictors in grassland and arable ecosystems (Table 2).

Further assessment of model performance was performed through an external validation step comparing the mean of observed and predicted fluxes in the test dataset (n=~140 per flux). The mean measured CO$_2$ and CH$_4$ fluxes were similar to the predicted carbon fluxes across all the data categories (RS, SP, CD). In contrast to the carbon fluxes, the measured N$_2$O fluxes were significantly lower than the predicted fluxes in autumn (Figure A1 in Appendices).

261 **Table 2:** List of predictor variables and the performance of the selected RF models using either remote sensing (RS), soil physico-
262 chemical parameters (SP), or combined (remote sensing and soil parameters) data. The model selection was made after a cross-
263 validation (10-fold) step whereby the model's predictive power was tested based on unseen data to avoid overfitting.

Flux type	Land use	Category	Predictor variables	10-fold cross validation		
				R^2	RMSE	MAE
SR/ER-CO_2-C (mg m^{-2} h^{-1})	Forest (SR)	Remotely-sensed data (RS)	NDVI, GNDVI, NDMI	0.45	1.76	1.55
	Grassland (ER)		NDVI, GNDVI, NDMI	0.46	1.88	1.61
	Arable (ER)		Elevation, NDVI, GNDVI, NDMI	0.73	1.76	1.58
CH_4-C (µg m^{-2} h^{-1})	Forest		Aspect, NDVI, GNDVI	0.14	46.38	36.15
	Grassland		Elevation, TPI, NDVI, NDMI	0.15	29.23	21.53
	Arable		GNDVI, NDMI	0.35	50.79	34.72
N_2O-N (µg m^{-2} h^{-1})	Forest		NDVI, GNDVI, NDMI	0.13	18.46	18.62
	Grassland		NDVI, GNDVI, NDMI	0.13	20.00	18.26
	Arable		GNDVI, NDMI	0.53	20.00	18.50
SR/ER-CO_2-C (mg m^{-2} h^{-1})	Forest (SR)	Soil physico-chemical parameters (SP)	Soil moisture, pH, NH_4-N, DOC	0.49	1.72	1.53
	Grassland (ER)		Soil moisture, NH_4-N, TDN	0.54	1.79	1.55
	Arable (ER)		Soil moisture, SN	0.63	1.94	1.70
CH_4-C (µg m^{-2} h^{-1})	Forest		Soil temperature, soil moisture, pH, NO_3-N, silt	0.16	44.29	33.87
	Grassland		Soil moisture, pH, NO_3-N, DOC, CN, clay	0.29	25.59	18.62
	Arable		DOC, CN	0.29	44.51	32.65
N_2O-N (µg m^{-2} h^{-1})	Forest		Soil moisture, NO_3-N, NH_4-N	0.15	18.49	18.65
	Grassland		Soil moisture, NH_4-N, CN, clay	0.22	18.02	18.37
	Arable		Soil moisture, NO_3-N, SN, CN	0.46	18.28	18.48
SR/ER-CO_2-C (mg m^{-2} h^{-1})	Forest (SR)	Combined data (CD)	NDVI, GNDVI, NDMI, soil moisture, NH_4-N, DOC	0.57	1.64	1.48
	Grassland (ER)		GNDVI, soil moisture, NH_4-N	0.57	1.76	1.54
	Arable (ER)		NDVI, GNDVI, soil moisture, SN	0.78	1.68	1.51
CH_4-C (µg m^{-2} h^{-1})	Forest		Aspect, soil temperature, soil moisture, NO_3-N	0.21	43.50	34.58
	Grassland		Soil moisture, pH, NO_3-N, CN, clay	0.30	25.38	18.29
	Arable		GNDVI, NDMI, CN	0.31	47.59	33.30
N_2O-N (µg m^{-2} h^{-1})	Forest		Soil moisture, NO_3-N, NH_4-N	0.15	18.49	18.65
	Grassland		NDVI, soil moisture	0.25	18.05	18.37
	Arable		NDVI, GNDVI, NDMI, soil moisture	0.56	18.36	18.52

264

3.2 Observed versus predicted GHG fluxes

266 The measured and predicted GHG fluxes for all the sampling points had significant (p<0.001) linear
267 relationships (Figure 3). The model predictions of SR/ER_CO_2 fluxes were better (r^2; 0.49 – 0.67) than for soil CH_4
268 (r^2; 0.39 – 0.46) or N_2O (r^2; 0.34 – 0.43) flux predictions across the three input datasets. Based on the estimated
269 slopes, the predicted values were 35 – 46% lower than the measured values for SR/ER_CO_2 fluxes. Compared to
270 CO_2, the CH_4 and N_2O predicted fluxes were lower (CH_4 53 – 58%; N_2O 60 – 65%) than the measured fluxes,

271   primarily due to the underestimation of high fluxes. Based on r^2 values, the performances of the different predictor

272   datasets were in the order of CD>RS>SP for carbon fluxes and CD>SP>RS for N_2O fluxes (Figure 3).

273
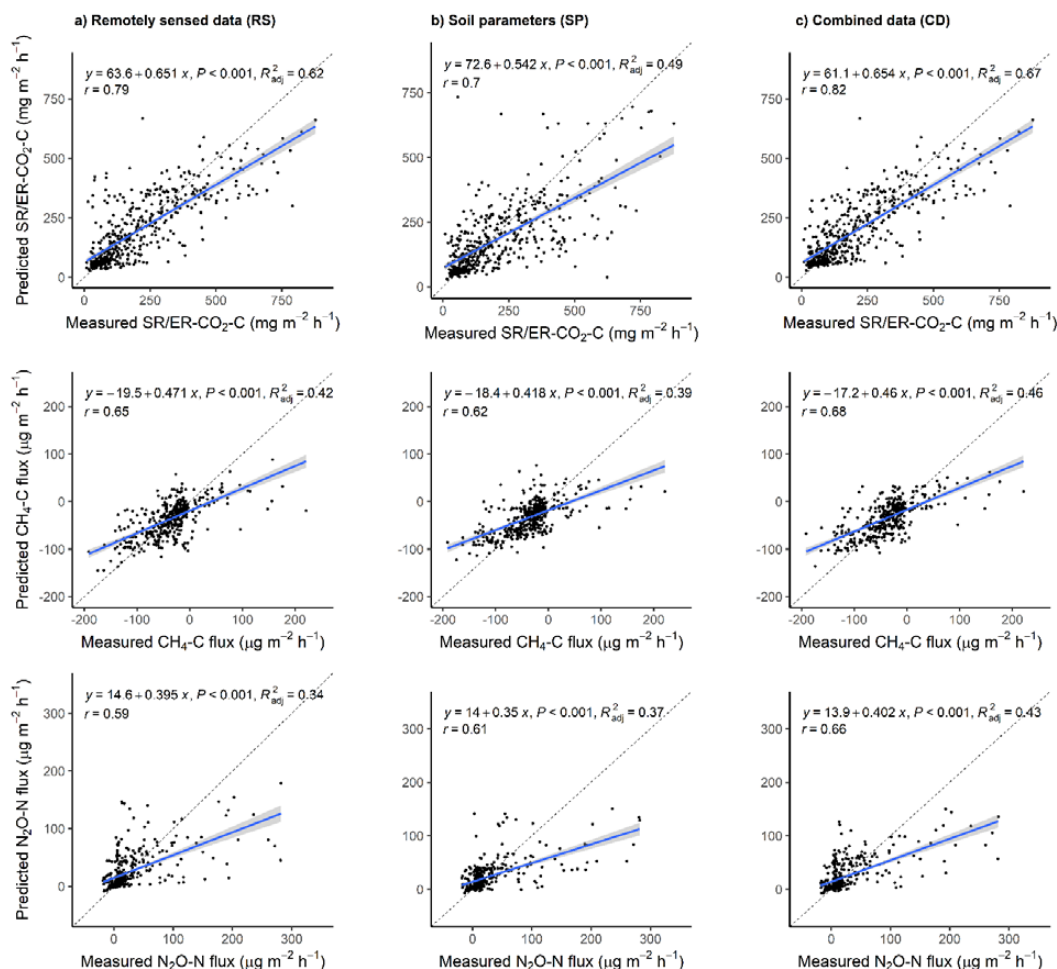
Figure 3: Linear regressions (with 95% confidence bands) of the measured and predicted GHG fluxes using remotely sensed data (RS), soil physico-chemical parameters (SP), and combined data (CD). GHG fluxes from all the sampling locations were considered in this regression analysis. The dotted line represents the 1:1 line.

3.3 Spatio-temporal variation in modeled landscape-scale fluxes

278   Predicted landscape fluxes for the summer and autumn seasons ranged from +27.7 – +733.3 mg m^{-2} h^{-1} for

279   CO_2-C, -148.4 – +89.4 µg m^{-2} h^{-1} for CH_4-C, and from -8.8– +189.9 µg m^{-2} h^{-1} for N_2O, and did not differ much in

280   dependence of the input dataset used (RS, SP, or CD) (Table B6 in Appendices). However, the predicted flux ranges

281   for the landscape were narrower than the measured fluxes, which ranged from 8.7 to 877.0 mg m^{-2} h^{-1} for CO_2-C,

282   from -214.1 – +221.2 µg m^{-2} h^{-1} for CH_4-C and from -18.1 – +281.8 µg m^{-2} h^{-1} for N_2O-N. Since the CD dataset

283   revealed models with better predictions for all GHG fluxes than the RS and SP datasets, we used GHG fluxes

284   predicted from CD predictors for seasonal and land use comparisons.

285   Most of the landscape area (99.2%) had higher SR/ER_CO_2 fluxes in summer than in autumn, with a small

286   proportion of arable and grassland ecosystems having an opposite trend. Around 76% of the landscape also had

287   higher N_2O fluxes in summer than in autumn. The remaining landscape area (24%) had higher N_2O fluxes in autumn

288   than in summer, particularly in forested areas. CH_4 uptake rates were lower in summer than autumn in most of the

289   landscape (63%), especially in arable and grassland soils. However, an opposite trend was found for about 37% of

290   the landscape area, dominated by forests, where CH_4 uptake rates were lower in autumn than in summer (Figure 4c).

291   High spatial heterogeneities (within short distances of <2 m) of the predicted landscape fluxes were

292   observed in each land use. Overall, spatial variations were more prominent in summer than in autumn (Figure 4;

293   Table B6 in Appendices). The spatial variability of SR/ER_CO_2 fluxes was higher (with a range of up to 2.6-folds)

294   on arable soils than forest and grassland soils, with multiple patches of low fluxes surrounded by high fluxes. CH_4

295   fluxes on arable lands were also heterogenous, with the soils acting as CH_4 sinks and sources within a few meters,

296   especially during summer (Figure 4a). For N_2O fluxes, high spatial heterogeneities were observed on grassland soils

297   in summer, as N_2O uptake and emission of the same or even higher order of magnitude occurred at neighboring

298   pixels. Arable soils in autumn were also highly heterogeneous, with patches of high N_2O fluxes surrounded by low

299   fluxes (Figure 4b).
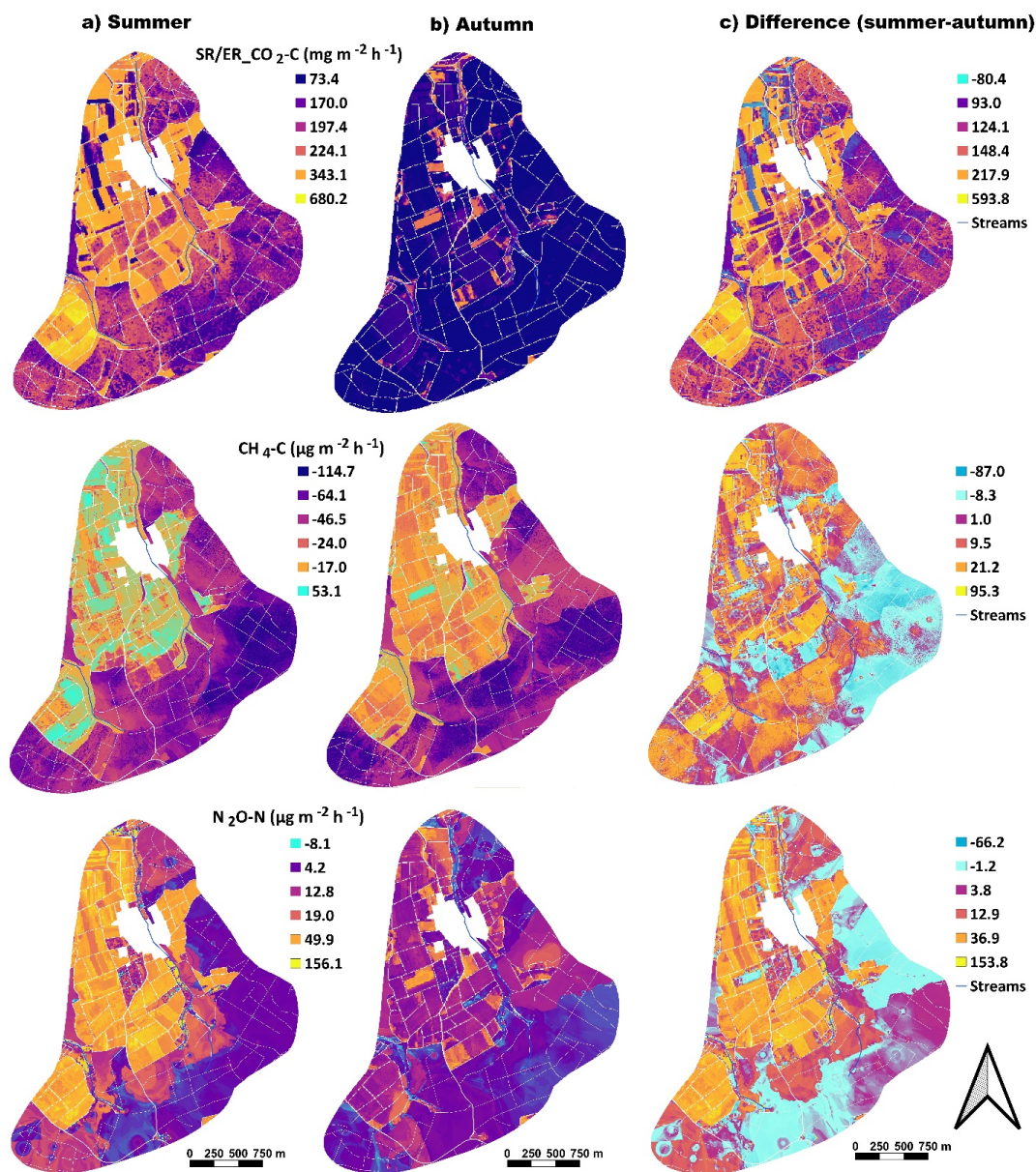
Figure 4: Landscape maps of SR/ER_CO₂, CH₄, and N₂O for (a) summer, (b) autumn seasons, and (c) the difference maps showing the variation of the autumn from the summer fluxes. The surface fluxes were predicted using RF models trained with combined (remote-sensing and site-measured soil parameters) data (CD; Table 2).

3.4 Hot spots and cold spots

The hot and cold spots of the GHG fluxes were identified from the average (summer and autumn) upscaled landscape fluxes (Figure 5a). Using equation 4, the SR/ER_CO$_2$ and N$_2$O spatial hot spots had threshold values >231.5 mg CO$_2$-C m^{-2} h^{-1} for CO$_2$ and >36.8 µg N$_2$O-N m^{-2} h^{-1} for N$_2$O. These hot spots covered a relatively small portion (~16.7%) of the landscape, yet they played a significant role, especially the N$_2$O hot spots which accounted for 42% of the landscape fluxes. Around 29% of the total SR/ER_CO$_2$ landscape flux emanated from the hot spot areas (Figure 5). Overall, the SR/ER_CO$_2$ and N$_2$O hot spots were mainly located on arable lands (77.0% and 94.5%, respectively) and grasslands (22.9% and 5.5%, respectively). Compared to the SR/ER_CO$_2$ and N$_2$O hot spots, the hot and cold spots of CH$_4$ uptake were observed in smaller regions (3.1% and 7.3%) of the landscape with high soil CH$_4$ uptake rates (>87.3 µg CH$_4$-C m^{-2} h^{-1}) and low soil CH$_4$ uptake rates (<3.4 µg CH$_4$-C m^{-2} h^{-1}). The CH$_4$ uptake hot spots, exclusively on the forested soils, offset 8% of the landscape CH$_4$ fluxes (Figure 5). The cold spots occupied 7% of the landscape and were primarily on arable soils (99.6%), accounting for 2% of the landscape's CH$_4$ emissions.

Common hot spots, with overlapping areas with elevated GHG emissions (i.e., SR/ER_CO$_2$ and N$_2$O hot spot areas and CH$_4$ uptake cold spot areas), were mainly on arable soils (99.87%), with few located in grasslands (0.12%) and forests (0.01%). Overall, these patches covered 1.5% of the landscape area and contributed 5%, 1%, and 8% of the SR/ER_CO$_2$, CH$_4$, and N$_2$O emissions within the landscape (Figure A2 in Appendices). Based on field observations of the sampling sites (n=14) in the common hot spots, the sites at arable lands were either cropped with barley or wheat. These arable common hot spots also had higher soil moisture content and NO$_3$ concentrations than the average values recorded at all the other sampling locations. The common hot spots in the forest were found along the riparian zones if either nitrogen-fixing alder trees were present or if grazed by cattle. Soil moisture (%), DOC, NO$_3$, and NH$_4$ concentrations at these sites were also higher than mean values across all sampling points. The grassland common hot spot regions were densely covered by nitrogen-fixing clover, with some located along the riparian zones (Figure A3; Table B7 in Appendices).

Comparison of the GHG emission hot spots in summer and autumn using season-specific thresholds revealed significant shifts in their geo-locations between the two seasons (Figure A4 in Appendices). SR/ER_CO$_2$ hot spot regions expanded by 46% from summer to autumn, even though the emissions from the former season were higher. Unlike CO$_2$, N$_2$O emission hot spots and CH$_4$ uptake cold spots contracted by 23% and 86%, respectively, from summer to autumn.
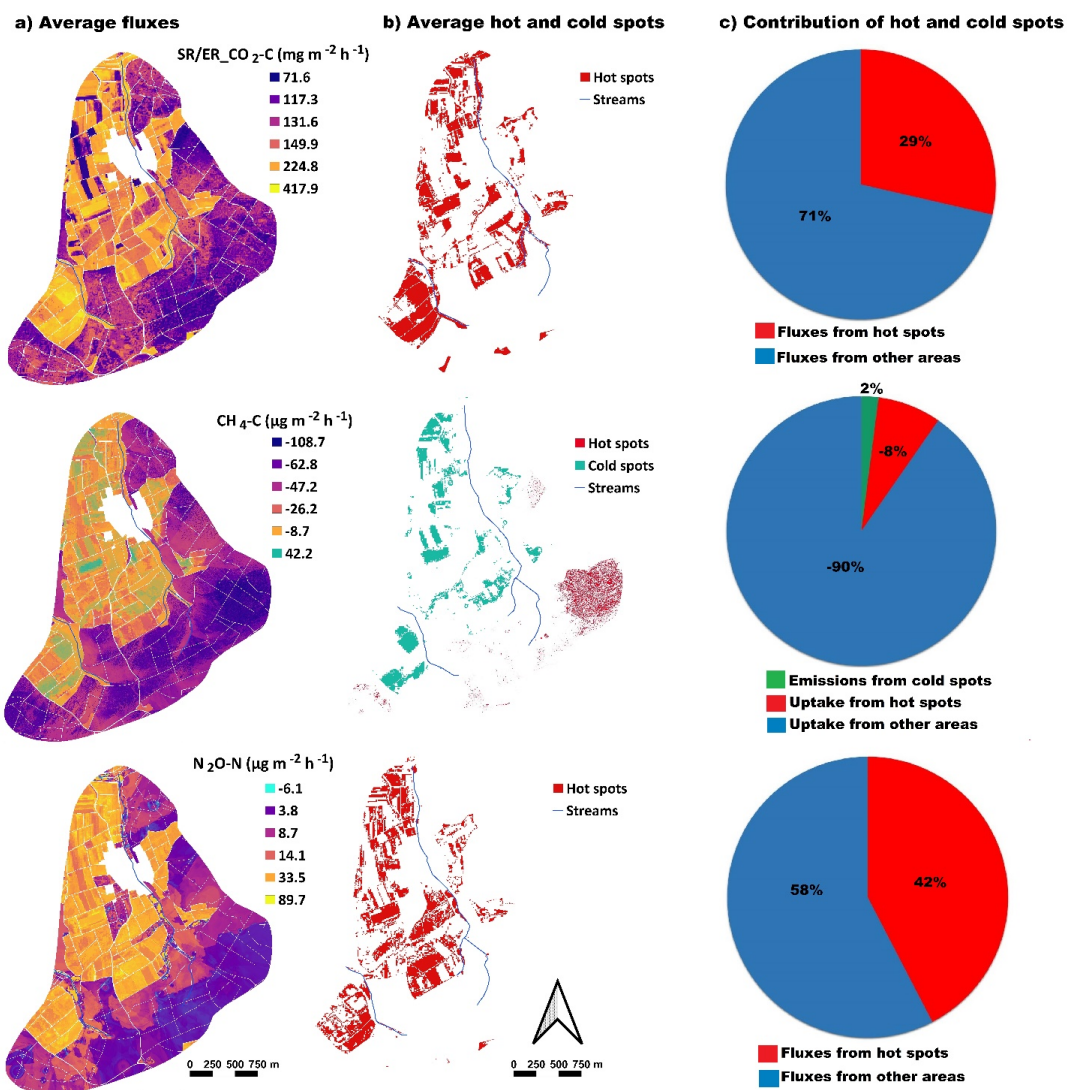
Figure 5: Maps showing (a) the average GHG fluxes and (b) the average hot spot and cold spot regions on the landscape for the summer and autumn seasons. The pie charts show the contribution (%) of hot and cold spots to total landscape fluxes. For this analysis, landscape fluxes were predicted using the combined data (CD; Table 2; Figure 3).

3.5 Comparison of upscaling approaches

Seasonal differences in spatial patterns and magnitudes of GHG fluxes were observed for upscaled fluxes using either RF modeling or mean values of measured fluxes. In both approaches, the SR/ER_CO_2 and N_2O landscape fluxes were an order of magnitude higher in summer than in autumn. The CH_4 uptake rates were higher in autumn than in summer but within the same order of magnitude. In summer, the landscape-scale SR/ER_CO_2 and N_2O fluxes estimated using the area-weighted average approach were 26% and 50% higher than the RF-modelled

343   fluxes. The contrary was observed in autumn, where the later methodology produced slightly (4% and 11%) higher

344   fluxes than the area-weighted mean estimates.

345   The entire landscape CH_4 uptake estimates for autumn using the area-weighted mean were 16% higher than

346   the modeled estimates. Contrary to autumn, the area-weighted mean approach had slightly lower estimates of CH_4

347   uptake than the modeling approach in summer. Additionally, the CH_4 surface flux estimates for the whole arable land

348   in summer were net sinks (-0.9 CH_4-C g h^{-1}) using the RF modeling approach contrary to the net sources (15.5 CH_4-

349   C g h^{-1}) estimated by the area-weighted mean method. Overall, the total landscape fluxes estimated using the area-

350   weighted mean approach had up to two orders of magnitude higher uncertainty (standard error) than the modeled

351   landscape fluxes (Figure 6).
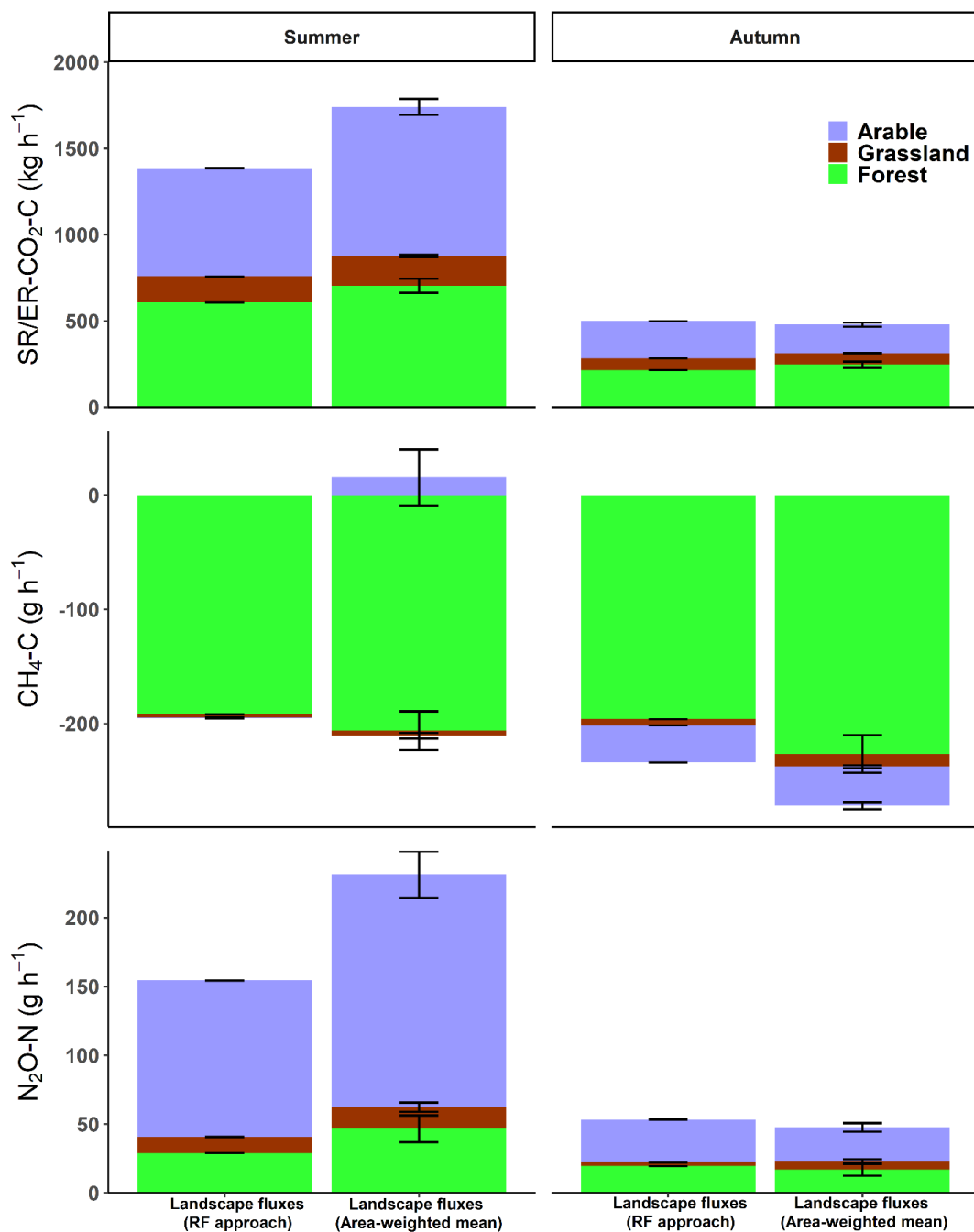
Figure 6: The total landscape fluxes (+SE) predicted using random forest (RF) models (with combined dataset) and the fluxes estimated using the area-weighted mean approach where the average point-measured fluxes were multiplied by the landscape area.

4. Discussion

4.1 Efficiency of in-situ soil parameters and remote-sensing data in upscaling GHG fluxes

357   Our study showed that remotely-sensed (RS) data and measured soil parameters (SP) could effectively
358 upscale soil-atmosphere CO_2, N_2O, and CH_4 fluxes from point chamber measurements across a heterogenous
359 landscape with mixed land uses. The improved prediction performance of the combined data (CD) sources indicates
360 the importance of incorporating controls of soil GHG fluxes that are remotely sensed and ground-based field
361 observations. The prediction models in this study suggested that the Sentinel-2-derived indices (NDVI, GNDVI, and
362 NDMI) were more effective predictors than the DEM-derived terrain attributes (elevation, slope, aspect, TWI, and
363 TPI). This finding is supported by the appearance of the Sentinel-2-derived indices in the prediction models of the
364 three GHGs, contrary to only one DEM index (aspect) that appeared in the CH_4 flux prediction models for the forest
365 ecosystem. The minor role of DEM indices in this study can be attributed to the relatively flat terrain of our study
366 landscape (Figure 1b) and is further backed by the lack of spatial variation in the measured GHG fluxes with slope,
367 yet slope was considered during site stratification (Wangari et al., 2022). Another possible explanation could be that
368 soil wetness, a common predictor of all the GHG fluxes across the landscape, was better represented by the site-
369 measured soil moisture content and the NDMI index (vegetation water content), than any of the DEM terrain
370 attributes, including the TWI that focuses on moisture conditions, as they lack a temporal dimension.

371   Compared with other studies that have upscaled GHG fluxes using the random forest algorithm, we
372 considered more site-measured data on soil parameters, all three GHG fluxes, and different land uses (Table 3). The
373 prediction accuracies of soil respiration for our mixed forest ecosystem (3.3 km^2) were slightly better than those
374 reported for a smaller forested headwater watershed (0.12 km^2) in Maryland, USA (Warner et al., 2019). Our CH_4
375 prediction performance for forest soils was comparable to those of a boreal forest landscape (Vainio et al., 2021).
376 However, our CH_4 prediction performance was up to 3.6-folds lower than those of a forested headwater watershed
377 and peatland soils, which can be attributed to higher and more homogenous CH_4 production in such ecosystems
378 (Warner et al., 2019; Räsänen et al., 2021). Our CH_4 and N_2O model prediction accuracies for arable soils were
379 better than those for arable soils in New South Wales, Australia, which only considered input data from ground-
380 based sensors such as soil pH and clay content (McDaniel et al., 2017). Nevertheless, caution has to be taken when
381 interpreting any conclusions from these study comparisons due to the limitations of different model validation
382 techniques, different predictor variables used for modeling, and the different ecosystems and spatial scales of
383 measurement and predictions.

4.2 Seasonal variability of landscape fluxes

385   The GHG fluxes predicted by the RF model in this study revealed seasonal trends of up to 3-fold higher
386 CO_2 and N_2O fluxes in summer and 1.2-fold higher CH_4 uptake in autumn, which were also evident in the measured
387 fluxes at the sampling points (Wangari et al., 2022). These trends can be attributed to seasonal changes in soil
388 parameters and vegetation within the landscape that were well captured by the measured soil parameters and
389 Sentinel-2-derived indices in the prediction models. The higher soil moisture, mineral nitrogen, and vegetation cover
390 observed during the summer growing season enhanced the respiration rates (SR/ER_CO_2) and N_2O emissions,

391   particularly in arable ecosystems, which were flux hot spots for both gases. Root respiration of growing plants can
392   also enhance N_2O production through denitrification by creating anaerobic conditions and supplying labile exudates
393   to denitrifying microbes (Butterbach-Bahl & Dannenmann, 2011; Malique et al., 2019). Previous studies have shown
394   that higher mineral nitrogen and soil moisture content can enhance N_2O production in soils through an increased
395   supply of substrates and the creation of anaerobic conditions that enhance denitrification rates (Barton et al., 1999;
396   Ciarlo et al., 2006; Butterbach-Bahl et al., 2013). The lower CH_4 uptake rates in summer can be primarily explained
397   by the observed higher soil moisture content, which has been previously reported to hinder CH_4 oxidation by slowing
398   down gas (atmospheric CH_4) diffusion in soils (Le Mer & Roger, 2001).

399   The high-resolution (1 m pixel size) scaled-up fluxes could also identify detailed temporal patterns of the
400   GHG fluxes across the landscape, thus, revealing trends that were otherwise undetectable in the aggregated measured
401   (point) fluxes. To illustrate, parts of the landscape (24% and 37%) showed even opposite trends of higher N_2O fluxes
402   and lower CH_4 uptake rates in autumn, and these areas were predominantly in the forested ecosystem. Such fine-
403   scale patterns of GHG fluxes result from land use-specific local effects depending on the season. For example,
404   decaying fallen leaves during autumn can favor denitrification in forest soils but not in grassland or arable
405   ecosystems. The higher CH_4 uptake rates in summer could be due to the increased exposure of some forest soils to
406   the sun leading to drier and warmer soils that promote CH_4 oxidation (Steinkamp et al., 2000). This finding is
407   supported by the importance of aspect as a predictor of landscape CH_4 fluxes in the forest ecosystem, which
408   influences the amount of incoming radiation an area receives.

4.3 Importance of hot spots and cold spots of landscape-scale GHG fluxes

410   The high spatial resolution of our predicted GHG fluxes enabled the identification of areas across the
411   landscape that functioned as hot spots (of soil CH_4 uptake, SR/ER_CO_2, and N_2O) or cold spots of soil CH_4 uptake.
412   Based on field observations and analyses of important predictor variables, the existence of these hot and cold spots
413   was primarily driven by human activities such as fertilizer application, crop growing and tillage, and landscape
414   environmental parameters related to seasonality and proximity to riparian areas. This finding is supported by the
415   primary association of the SR/ER_CO_2 and N_2O hot spots and CH_4 uptake cold spots within arable ecosystems since
416   these systems showed higher soil mineral nitrogen concentrations than grassland and forest soils. The hot spots of
417   SR/ER_CO_2 and N_2O observed on the grassland ecosystem can be attributed to the primary location of grasslands
418   along the riparian areas. Increased soil moisture values, a key characteristic of the riparian regions, has also been
419   reported to drive elevated soil GHG fluxes (Kaiser et al., 2018; Vainio et al., 2021).

420   Spatial hot spots of SR/ER_CO_2 and N_2O played a crucial role in determining total landscape fluxes,
421   accounting for up to 42% of the total predicted landscape fluxes, despite their relatively low (~16%) coverage area.
422   Such high contributions suggest that failure to capture these hot spots results in large uncertainties in landscape GHG
423   flux estimates. Overall, the contribution of the hot spot areas (of CO_2, N_2O, and CH_4 emissions) to the landscape
424   fluxes decreased in the order of $N_2O>CO_2>CH_4$. This finding emphasizes the importance of capturing the N_2O hot
425   spots and improving the spatial coverage of N_2O measurements, as it can introduce enormous uncertainty in
426   landscape fluxes. A similar finding emphasizing the importance of N_2O flux heterogeneities has been concluded in a

427   previous study, which recorded more sampling locations required for improved N_2O flux estimates than CO_2 and

428   CH_4 at a landscape scale (Wangari et al., 2022).

429   Identifying common patches with elevated emissions of the three GHGs can inform priority areas for

430   implementing localized mitigation measures within a landscape. These common patches covered only 1.5% of our

431   landscape (~0.2 km^2) and had the highest GHG fluxes contributing around 5%, 1%, and 8% of the landscape CO_2,

432   CH_4, and N_2O emissions. The location of these patches primarily (99.9%) on arable land emphasized the significant

433   role of focusing on mitigating GHG fluxes from arable soils. The mitigation strategies may include adjusting the

434   fertilizer application rates, especially in specific areas that hold more water, probably due to topographical or soil

435   conditions (e.g., Hassan et al., 2022). This finding is further supported by the high soil moisture content measured at

436   the sampling sites within the common patches of elevated GHG fluxes. In contrast to hot spot regions of elevated

437   GHG emissions, CH_4 uptake hotspots inform future mechanisms for leveraging the GHG sink ability of soils, such as

438   expanding local forests. This finding is supported by uptake hot spots identified on forest soils in this study,

439   offsetting 8% of the total landscape CH_4 flux. The expansion of forested areas will also likely have a much higher

440   mitigation impact via CO_2 sequestration. Although some of the above strategies are currently applied at broader

441   scales (1 km^2), localized mitigation strategies may be required at smaller scales (<100 m^2), especially at highly

442   heterogeneous landscapes with a high variability of agricultural practices. We also found significant shifts in the geo-

443   locations of hotspot regions between summer and autumn, suggesting that seasonal changes in land management and

444   soil conditions may also lead to a temporal expansion or contraction of the hot spot regions. This finding further

445   emphasizes the need for time-based mitigation strategies, such as considering fertilizer application times, which not

446   only target the spatial hotspots but also consider the temporal patterns that result in peak emissions (e.g., Wagner-

447   Riddle et al., 2020).

448   **4.4 Comparison of upscaling approaches**

449   Contrary to the area-weighted upscaling approach of spatial aggregation of chamber fluxes (Webster et al.,

450   2008; Molodovskaya et al., 2011; Rosenstock et al., 2016), random forest modeling allowed us to estimate the entire

451   spatial distributions of the fluxes at high spatial resolution (1 m pixel size), capturing both cold spots and hot spots.

452   In agreement with our hypotheses, the landscape fluxes were either over or under-estimated by the area-weighted

453   average approach compared to the RF modeling approach. The overestimated landscape CO_2 and N_2O fluxes by up

454   to 50% during the peak summer season suggest an overrepresentation of the high fluxes measured at most of the

455   sampling points, resulting in elevated mean and upscaled fluxes. Furthermore, landscape CH_4 uptake rates were

456   overestimated during the peak autumn season. Previous studies have also observed a similar trend of elevated mean

457   CH_4 uptake rates at measured sites, which they attributed to the over-representation of high uptake rates during the

458   peak uptake seasons (Warner et al., 2019). Conversely, the underestimation of CO_2, N_2O, and CH_4 uptake, especially

459   on arable soils, coincided with the low flux season, implying reduced mean fluxes due to the overrepresentation of

460   the low fluxes. An alternative explanation of the differences in landscape flux estimates from both approaches could

461   be the underestimation of high fluxes by the RF models, which we also found in our study. However, the landscape

462   means of RF predicted and measured fluxes from 30% of our sampled sites were primarily similar (Figure A1 in

463   Appendices), suggesting that the lack of spatial representation of all hot and cold spots by the area-weighted mean

464   approach rather than the inability of the RF models to reproduce high values accounted for the findings above.

465   Collectively, our results illustrated that the representativeness of landscape fluxes using aggregated chamber

466   fluxes might be influenced by the spatial and temporal heterogeneity of the fluxes. This finding aligns with previous

467   results on the required number of chamber measurement locations for reliable landscape fluxes that varied with land

468   use and season (Warner et al., 2019, Wangari et al., 2022). The high (50%) overestimation of landscape N_2O fluxes

469   suggested the higher sensitivity of reliably estimating N_2O fluxes using the (aggregated means) conventional method.

470   Previous studies have also emphasized the importance of N_2O fluxes in constraining uncertainties in landscape flux

471   quantification (e.g., Wangari et al., 2022). Compared to the suggested way of lowering landscape-scale flux

472   uncertainties in the conventional estimates by increasing the number of chamber measurements within a landscape

473   (Wangari et al., 2022), the modeling approach can be a less resource-intensive alternative.

474   Combining high-resolution remote sensing data and measured soil parameters to upscale the chamber fluxes

475   reduced the biases and the aforementioned landscape-scale flux uncertainties. The reduced uncertainties in the

476   modeled landscape fluxes can be attributed to the relation of multiple underlying controls of soil GHG fluxes, which

477   have high seasonal and spatial variability. Remote sensing datasets have unlimited spatial extents with high spatial

478   resolution and thus allowing reliable prediction of spatially continuous fluxes that can capture the cold and hot spots

479   over different seasons across heterogeneous landscapes (Warner et al., 2019; Räsänen et al., 2021). This study's high

480   spatial resolution upscaling (1 m pixel) enabled capturing small-scale variabilities in GHG fluxes within short

481   distances, which would have been missed out with coarser resolution upscaling. Upscaling at a finer resolution was

482   especially relevant due to the heterogeneous nature of our study landscape, related to different land uses, soil types,

483   and slope positions.

5. Conclusions

485   This study demonstrated the potential of improved prediction performance when combining field-based

486   measurements of soil parameters with remotely-sensed data in scaling up flux (chamber) measurements from

487   stratified sites. Among the remotely-sensed predictors, Sentinel-2 indices played a more significant role than DEM-

488   derived attributes in upscaling the GHG fluxes across our relatively flat landscape terrain. The high-resolution (1 m

489   pixel size) scaled-up fluxes effectively revealed fine-scale (within a few meters) hot and cold spots of GHG fluxes

490   across a mixed land use landscape. The N_2O hot spots were more significant sources of GHGs as they contributed

491   42% of the landscape N_2O fluxes compared to SR/ER_CO_2 and CH_4 emission hotspots, which accounted for 29%

492   and 2% of the landscape CO_2 and CH_4 emissions, respectively. Arable soils, which had higher N_2O fluxes, also had

493   patches with elevated emissions of the three GHGs, especially in areas with high soil moisture content. These

494   findings emphasize the importance of targeted local mitigation measures, especially for agricultural soils, in

495   mitigating landscape GHG fluxes. Compared to RF upscaling, the area-weighted average approach lacked detailed

496   spatiotemporal patterns of landscape fluxes, which can prevent targeted mitigation measures to some extent.

Table 3: Comparison of other that have upscaled landscape fluxes using the random forest algorithm.

Study area	Landscape area (km²)	Number of sites	Predictor variables	Measurement period	Model algorithm	Type of validation	Prediction period	Land use	Flux	Model validation (r²)	Location	Reference
Gießen, Central Germany	5.85	268	o **DEM indices:** *elevation, slope, aspect, TWI & TPI*; o **Sentinel-2 indices:** *NDVI, GNDVI, & NDMI*; o **In-situ data:** *soil temperature, moisture, pH, bulk density, NO_3-N, NH_4-N, DOC, TDN, TN, TOC, CN, sand, silt & clay content*	July & September, 2020	Random forest	10-fold repeated cross-validation	Summer (Jul) and autumn (Sep)	Forest, grassland, arable; Forest, grassland, arable; Forest, grassland, arable	SR/ER_CO_2; CH_4; N_2O	0.57, 0.57, 0.78; 0.21, 0.30, 0.31; 0.15, 0.25, 0.56	50°30'4.23. N, 8°33'2.82. E	This study
Hyytiälä, southern Finland	0.1	60	o **DEM indices:** *slope, TWI, TRI & DTW*; o **In-situ data:** *soil moisture*	March-December 2013 & May-December 2014	Random forest	Distance-blocked leave-out cross-	Summer; Autumn	Forest (boreal)	CH_4	0.26; 0.39	61°510 N, 24°170 E	Vainio et al. (2021)
Maryland, USA	0.12	20	o **DEM indices:** *slope, aspect, TWI, flow line curvature, channel network base level, upslope accumulation area, etc.* o **In-situ data:** *soil temperature & moisture*	September 2014 - November 2016 (bimonthly)	Quantile regression forest	Model accuracy and prediction uncertainty assessment	Early summer: May-Jul; Late summer: Aug-Sep	Forest (headwater watershed)	CO_2 & CH_4	0.61, 0.50 (CO_2, CH_4); 0.40, 0.64 (CO_2, CH_4)	39°42' N, 75°50' W	Warner et al. (2019)
Pallas area, northern Finland	12.4	279	o **DEM indices:** *elevation, slope, aspect, TWI, TPI & DTW*; o **Sentinel-1 & 2 indices:** *NDVI, GNDVI, NDWI, etc.* o **In-situ data:** *soil moisture, vegetation (e.g., leaf area index)*	July 3 - 13, 2019	Random forest regressions and binary classifications	Random forest out-of-bag assessment	Summer (July)	Forest (peatland)	CH_4	0.76	67°57'–68°0 1' N, 24°10'–24°15' E	Räsänen et al. (2021)
Narrabri, New South Wales, Australia	0.16	>100	o **RSX-1 Gamma Detector variables:** *clay content, mineralogy, soil pH*; o **DUALEM-4 s Electromagnetic sensor variables:** *moisture, salinity, clay, thickness of the solum*	May 23-31, 2015	Quantile regression forest	Linear regression with validation dataset	Early summer (May)	Arable	CH_4 & N_2O	0.24, 0.07 (CH_4, N_2O)	149.82° E; 30.28° S	McDaniel et al. (2017)

497

498   **Appendices**

499   **Appendix A: Figures**

500
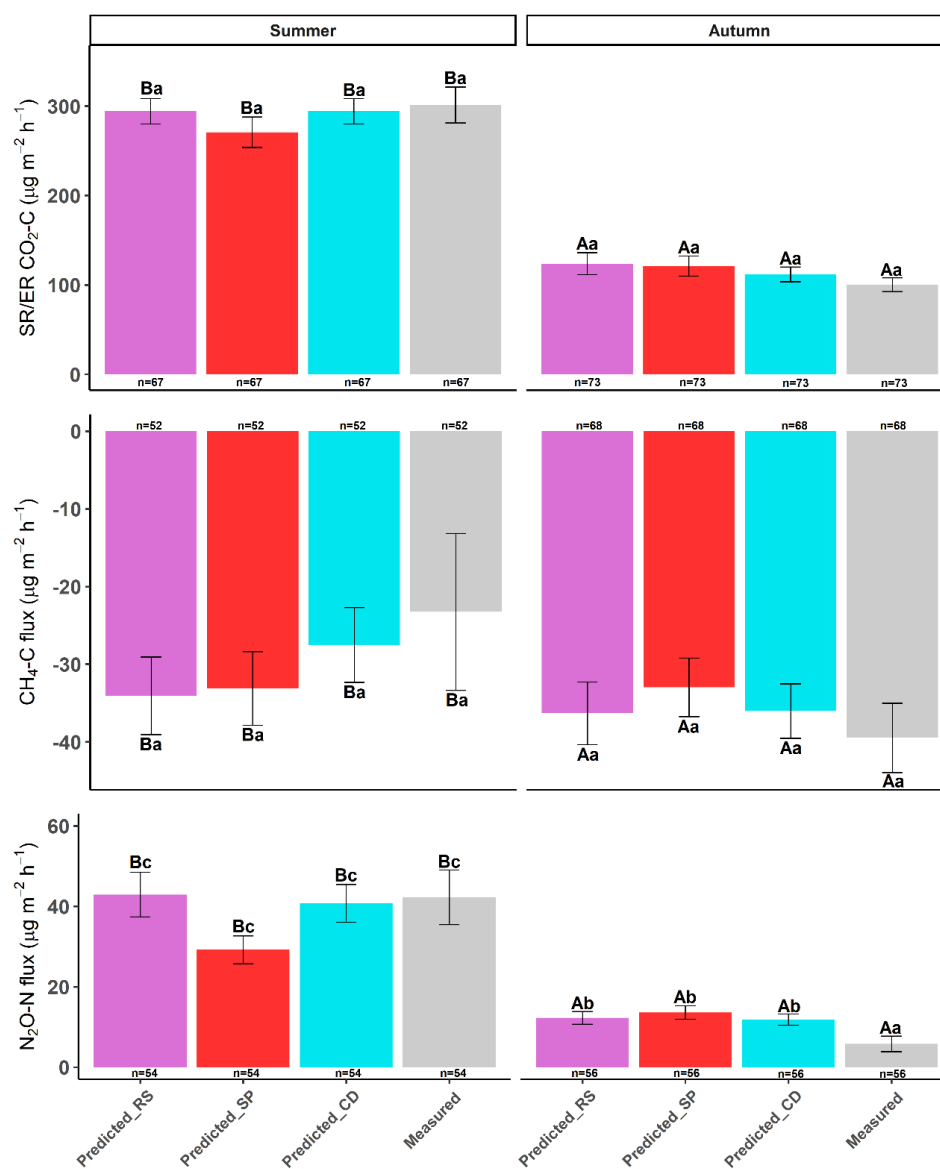
Figure A1: Bar graphs showing the mean fluxes (±SE) predicted using remote sensing (RS), soil properties (SP), and combined data (CD) and the measured fluxes at the sampling sites in the 30% model test dataset. The upper-case and lower-case letters indicate significant differences ($p < 0.05$) in the mean fluxes in the different seasons and across the measured and predicted fluxes.

504
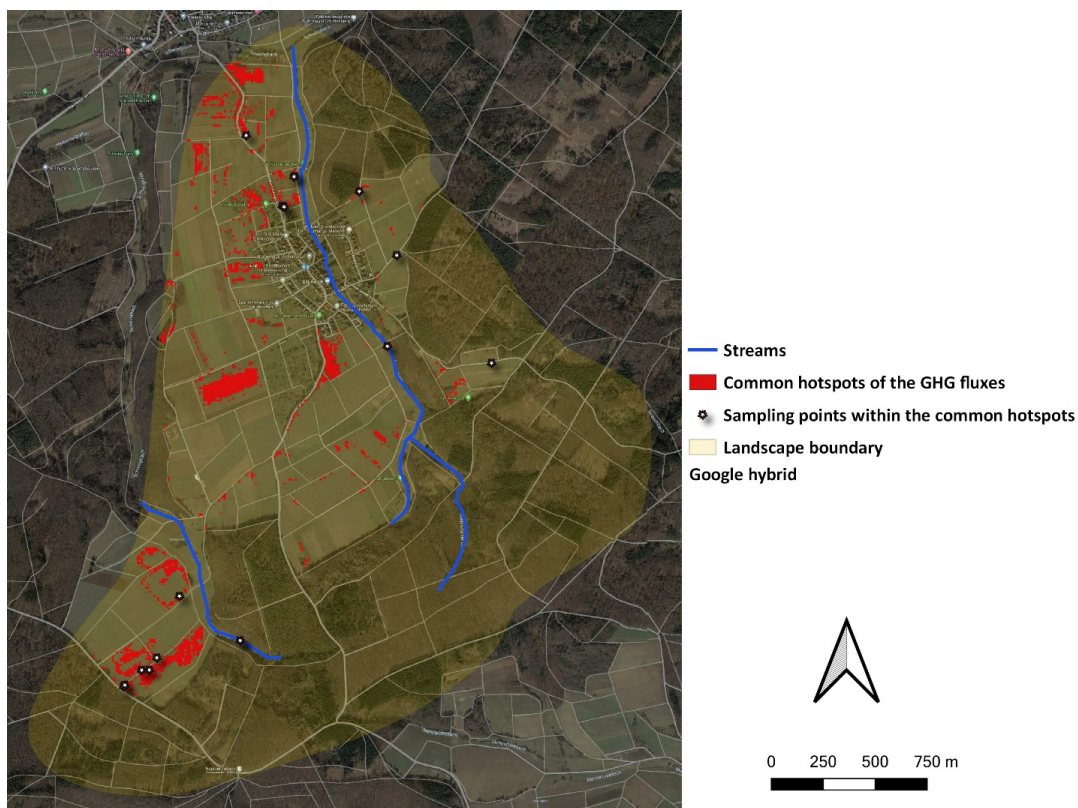
Figure A2: Map showing the common hotspot regions of the three GHG fluxes and the location of the measured sampling points
within these recurrent hotspots (Satellite Image downloaded from © Google Maps).

507

Figure A3: Clover (*Trifolium*) on grassland ecosystems.

509
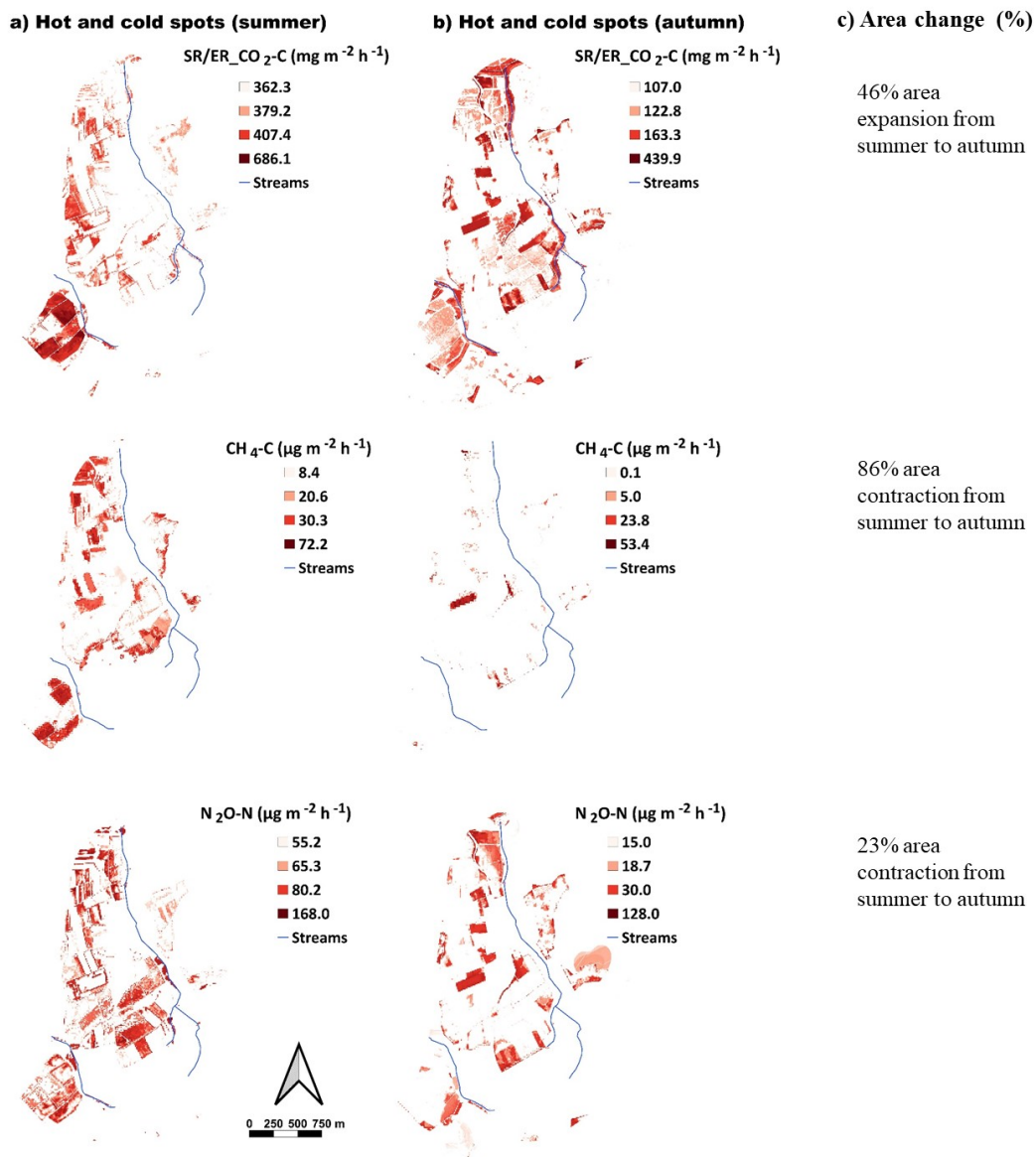
Figure A4: Maps showing the hot and cold spots of the (a) summer and (b) autumn seasons. These regions were defined using each season's specific threshold.

510
511

512 **Appendix B: Tables**

513 **Table B1 a, b, c:** Cross-validation results of different models developed for SR/ER-CO$_2$ fluxes in 1a) forest, 1b) grassland and 1c)
514 arable land using different predictors in the training dataset. Stepwise elimination of least important predictors was implemented.

B1a): Forest SR_CO$_2$-C flux			10-fold cross validation		
Category	**Predictor variables**	**mtry**	**RMSE**	**R^2**	**MAE**
Remote sensing	Elevation, slope, aspect, TWI, TPI, NDVI, GNDVI, NDMI	2	0.57	0.44	0.45
	Elevation, aspect, TWI, TPI, NDVI, GNDVI, NDMI	2	0.57	0.43	0.45
	Elevation, aspect, TPI, NDVI, GNDVI, NDMI	2	0.57	0.44	0.44
	Elevation, TPI, NDVI, GNDVI, NDMI	2	0.56	0.46	0.43
	Elevation, NDVI, GNDVI, NDMI	2	0.55	0.48	0.43
	NDVI, GNDVI, NDMI	2	0.56	0.45	0.44
	NDVI, GNDVI	2	0.59	0.42	0.45
	NDVI	2	0.63	0.36	0.49
Site measured soil parameters	Temperature, moisture, pH, bulk density, NO$_3$-N, NH$_4$-N, DOC, TDN, SOC, SN, CN, sand, silt, clay	8	0.54	0.50	0.42
	Temperature, moisture, pH, bulk density, NO$_3$-N, NH$_4$-N, DOC, TDN, SOC, SN, sand, silt, clay	7	0.53	0.51	0.41
	Temperature, moisture, pH, bulk density, NO$_3$-N, NH$_4$-N, DOC, TDN, SOC, SN, sand, silt	7	0.53	0.51	0.41
	Temperature, moisture, pH, bulk density, NH$_4$-N, DOC, TDN, SOC, SN, sand, silt	6	0.52	0.52	0.41
	Temperature, moisture, pH, bulk density, NH$_4$-N, DOC, TDN, SN, sand, silt	6	0.52	0.52	0.41
	Temperature, moisture, pH, bulk density, NH$_4$-N, DOC, TDN, sand, silt	5	0.53	0.52	0.41
	Moisture, pH, bulk density, NH$_4$-N, DOC, TDN, sand, silt	5	0.53	0.51	0.41
	Moisture, pH, NH$_4$-N, DOC, TDN, sand, silt	4	0.53	0.52	0.41
	Moisture, pH, NH$_4$-N, DOC, TDN, silt	2	0.52	0.53	0.41
	Moisture, pH, NH$_4$-N, DOC, TDN	2	0.53	0.51	0.42
	Moisture, pH, NH$_4$-N, DOC	2	0.54	0.49	0.42
	Moisture, NH$_4$-N, DOC	2	0.57	0.44	0.44
	Moisture, NH$_4$-N	2	0.57	0.44	0.45
	NH$_4$-N	2	0.60	0.41	0.48
Combined	Elevation, slope, aspect, TWI, TPI, NDVI, GNDVI, NDMI, temperature, moisture, pH, bulk density, NO$_3$-N, NH$_4$-N, DOC, TDN, SOC, SN, CN, sand, silt, clay	12	0.51	0.54	0.40
	Slope, aspect, TWI, TPI, NDVI, GNDVI, NDMI, temperature, moisture, pH, bulk density, NO$_3$-N, NH$_4$-N, DOC, TDN, SOC, SN, CN, sand, silt, clay	11	0.51	0.54	0.40
	Slope, aspect, TPI, NDVI, GNDVI, NDMI, temperature, moisture, pH, bulk density, NO$_3$-N, NH$_4$-N, DOC, TDN, SOC, SN, CN, sand, silt, clay	11	0.51	0.55	0.40
	Aspect, TPI, NDVI, GNDVI, NDMI, temperature, moisture, pH, bulk density, NO$_3$-N, NH$_4$-N, DOC, TDN, SOC, SN, CN, sand, silt, clay	10	0.51	0.55	0.40
	TPI, NDVI, GNDVI, NDMI, temperature, moisture, pH, bulk density, NO$_3$-N, NH$_4$-N, DOC, TDN, SOC, SN, CN, sand, silt, clay	10	0.51	0.55	0.40
	TPI, NDVI, GNDVI, NDMI, temperature, moisture, pH, bulk density, NO$_3$-N, NH$_4$-N, DOC, TDN, SOC, SN, CN, sand, silt	9	0.51	0.56	0.39
	TPI, NDVI, GNDVI, NDMI, temperature, moisture, pH, bulk density, NO$_3$-N, NH$_4$-N, DOC, TDN, SOC, SN, sand, silt	2	0.50	0.58	0.39
	NDVI, GNDVI, NDMI, temperature, moisture, pH, bulk density, NO$_3$-N, NH$_4$-N, DOC, TDN, SOC, SN, sand, silt	8	0.50	0.56	0.39
	NDVI, GNDVI, NDMI, temperature, moisture, pH, bulk density, NH$_4$-N, DOC, TDN, SOC, SN, sand, silt	2	0.49	0.59	0.39
	NDVI, GNDVI, NDMI, temperature, moisture, pH, bulk density, NH$_4$-N, DOC, TDN, SOC, SN, silt	2	0.49	0.60	0.38
	NDVI, GNDVI, NDMI, temperature, moisture, pH, NH$_4$-N, DOC, TDN, SOC, SN, silt	2	0.49	0.60	0.38
	NDVI, GNDVI, NDMI, temperature, moisture, pH, NH$_4$-N, DOC, TDN, SOC, silt	2	0.49	0.60	0.38
	NDVI, GNDVI, NDMI, moisture, pH, NH$_4$-N, DOC, TDN, SOC, silt	2	0.49	0.59	0.38
	NDVI, GNDVI, NDMI, moisture, pH, NH$_4$-N, DOC, TDN, silt	2	0.49	0.59	0.39
	NDVI, GNDVI, NDMI, moisture, pH, NH$_4$-N, DOC, TDN	2	0.50	0.57	0.39
	NDVI, GNDVI, NDMI, moisture, NH$_4$-N, DOC, TDN	2	0.50	0.57	0.39
	NDVI, GNDVI, NDMI, moisture, NH$_4$-N, DOC	2	0.50	0.57	0.39
	NDVI, GNDVI, moisture, NH$_4$-N, DOC	2	0.51	0.55	0.40
	NDVI, GNDVI, moisture, NH$_4$-N	3	0.51	0.55	0.40
	NDVI, moisture, NH$_4$-N	3	0.52	0.53	0.41
	NDVI, NH$_4$-N	2	0.52	0.54	0.41
	NH$_4$-N	2	0.60	0.41	0.48

515

Category	Predictor variables	mtry	RMSE	R^2	MAE
B1b): Grassland SR/ER_CO$_2$-C flux		10-fold cross validation			
Remote sensing	Elevation, slope, aspect, TWI, TPI, NDVI, GNDVI, NDMI	5	0.62	0.47	0.48
	Elevation, slope, aspect, TPI, NDVI, GNDVI, NDMI	2	0.62	0.48	0.48
	Elevation, aspect, TPI, NDVI, GNDVI, NDMI	2	0.62	0.48	0.47
	Elevation, aspect, NDVI, GNDVI, NDMI	2	0.61	0.49	0.47
	Elevation, NDVI, GNDVI, NDMI	2	0.62	0.48	0.46
	NDVI, GNDVI, NDMI	2	0.63	0.46	0.48
	NDVI, GNDVI	2	0.67	0.41	0.51
	GNDVI	2	0.72	0.36	0.54
Site measured soil parameters	Temperature, moisture, pH, bulk density, NO$_3$-N, NH$_4$-N, DOC, TDN, SOC, SN, CN, sand, silt, clay	8	0.56	0.56	0.43
	Temperature, moisture, pH, bulk density, NO$_3$-N, NH$_4$-N, DOC, TDN, SOC, SN, CN, sand, clay	7	0.56	0.57	0.43
	Temperature, moisture, pH, NO$_3$-N, NH$_4$-N, DOC, TDN, SOC, SN, CN, sand, clay	7	0.56	0.57	0.43
	Moisture, pH, NO$_3$-N, NH$_4$-N, DOC, TDN, SOC, SN, CN, sand, clay	6	0.56	0.56	0.43
	Moisture, pH, NO$_3$-N, NH$_4$-N, DOC, TDN, SOC, SN, CN, clay	6	0.56	0.57	0.43
	Moisture, pH, NO$_3$-N, NH$_4$-N, TDN, SOC, SN, CN, clay	5	0.56	0.57	0.42
	Moisture, pH, NO$_3$-N, NH$_4$-N, TDN, SOC, SN, CN	5	0.57	0.56	0.43
	Moisture, NO$_3$-N, NH$_4$-N, TDN, SOC, SN, CN	2	0.58	0.55	0.44
	Moisture, NH$_4$-N, TDN, SOC, SN, CN	2	0.58	0.54	0.44
	Moisture, NH$_4$-N, TDN, SN, CN	2	0.58	0.55	0.44
	Moisture, NH$_4$-N, TDN, CN	2	0.58	0.54	0.44
	Moisture, NH$_4$-N, TDN	2	0.58	0.54	0.44
	Moisture, NH$_4$-N	2	0.61	0.51	0.47
	Moisture	2	0.63	0.46	0.50
Combined	Elevation, slope, aspect, TWI, TPI, NDVI, GNDVI, NDMI, temperature, moisture, pH, bulk density, NO$_3$-N, NH$_4$-N, DOC, TDN, SOC, SN, CN, sand, silt, clay	12	0.55	0.58	0.41
	Elevation, slope, aspect, TWI, NDVI, GNDVI, NDMI, temperature, moisture, pH, bulk density, NO$_3$-N, NH$_4$-N, DOC, TDN, SOC, SN, CN, sand, silt, clay	11	0.55	0.59	0.41
	Elevation, slope, aspect, NDVI, GNDVI, NDMI, temperature, moisture, pH, bulk density, NO$_3$-N, NH$_4$-N, DOC, TDN, SOC, SN, CN, sand, silt, clay	11	0.55	0.59	0.41
	Elevation, aspect, NDVI, GNDVI, NDMI, temperature, moisture, pH, bulk density, NO$_3$-N, NH$_4$-N, DOC, TDN, SOC, SN, CN, sand, silt, clay	10	0.55	0.59	0.41
	Elevation, aspect, NDVI, GNDVI, NDMI, temperature, moisture, pH, bulk density, NO$_3$-N, NH$_4$-N, DOC, TDN, SOC, SN, CN, sand, clay	10	0.55	0.59	0.41
	Elevation, NDVI, GNDVI, NDMI, temperature, moisture, pH, bulk density, NO$_3$-N, NH$_4$-N, DOC, TDN, SOC, SN, CN, sand, clay	9	0.55	0.59	0.40
	Elevation, NDVI, GNDVI, NDMI, temperature, moisture, pH, NO$_3$-N, NH$_4$-N, DOC, TDN, SOC, SN, CN, sand, clay	9	0.55	0.59	0.41
	Elevation, NDVI, GNDVI, NDMI, moisture, pH, NO$_3$-N, NH$_4$-N, DOC, TDN, SOC, SN, CN, sand, clay	8	0.55	0.59	0.41
	Elevation, NDVI, GNDVI, NDMI, moisture, NO$_3$-N, NH$_4$-N, DOC, TDN, SOC, SN, CN, sand, clay	8	0.55	0.59	0.41
	Elevation, NDVI, GNDVI, NDMI, moisture, NO$_3$-N, NH$_4$-N, TDN, SOC, SN, CN, sand, clay	7	0.55	0.59	0.41
	Elevation, NDVI, GNDVI, NDMI, moisture, NO$_3$-N, NH$_4$-N, TDN, SOC, SN, CN, clay	7	0.55	0.58	0.41
	Elevation, NDVI, GNDVI, NDMI, moisture, NH$_4$-N, TDN, SOC, SN, CN, clay	6	0.55	0.59	0.41
	Elevation, NDVI, GNDVI, NDMI, moisture, NH$_4$-N, TDN, SOC, SN, CN	2	0.55	0.59	0.41
	NDVI, GNDVI, NDMI, moisture, NH$_4$-N, TDN, SOC, SN, CN	2	0.56	0.58	0.42
	NDVI, GNDVI, NDMI, moisture, NH$_4$-N, TDN, SOC, CN	2	0.55	0.59	0.41
	NDVI, GNDVI, NDMI, moisture, NH$_4$-N, TDN, CN	2	0.55	0.59	0.41
	NDVI, GNDVI, moisture, NH$_4$-N, TDN, CN	2	0.55	0.59	0.41
	NDVI, GNDVI, moisture, NH$_4$-N, CN	2	0.55	0.58	0.42
	NDVI, GNDVI, moisture, NH$_4$-N	2	0.55	0.59	0.42
	GNDVI, moisture, NH$_4$-N	2	0.56	0.57	0.43
	GNDVI, moisture	2	0.61	0.50	0.46
	Moisture	2	0.63	0.46	0.50

516

B1c): Arable SR/ER_CO$_2$-C flux		10-fold cross validation			
Category	Predictor variables	mtry	RMSE	R^2	MAE
Remote sensing	Elevation, slope, aspect, TWI, TPI, NDVI, GNDVI, NDMI	8	0.54	0.75	0.44
	Elevation, slope, aspect, TPI, NDVI, GNDVI, NDMI	7	0.54	0.75	0.44
	Elevation, slope, aspect, NDVI, GNDVI, NDMI	4	0.54	0.75	0.44
	Elevation, aspect, NDVI, GNDVI, NDMI	3	0.55	0.75	0.44
	Elevation, NDVI, GNDVI, NDMI	2	0.57	0.73	0.46
	NDVI, GNDVI, NDMI	2	0.59	0.72	0.46
	NDVI, GNDVI	2	0.60	0.71	0.47
	GNDVI	2	0.60	0.71	0.49
Site measured soil parameters	Temperature, moisture, pH, bulk density, NO$_3$-N, NH$_4$-N, DOC, TDN, SOC, SN, CN, sand, silt, clay	14	0.69	0.59	0.57
	Temperature, moisture, pH, bulk density, NO$_3$-N, NH$_4$-N, DOC, SOC, SN, CN, sand, silt, clay	13	0.69	0.60	0.56
	Temperature, moisture, pH, NO$_3$-N, NH$_4$-N, DOC, SOC, SN, CN, sand, silt, clay	12	0.68	0.61	0.56
	Temperature, moisture, pH, NO$_3$-N, NH$_4$-N, SOC, SN, CN, sand, silt, clay	11	0.67	0.61	0.55
	Temperature, moisture, pH, NH$_4$-N, SOC, SN, CN, sand, silt, clay	10	0.67	0.61	0.56
	Temperature, moisture, pH, NH$_4$-N, SOC, SN, CN, sand, clay	9	0.67	0.61	0.55
	Moisture, pH, NH$_4$-N, SOC, SN, CN, sand, clay	8	0.67	0.62	0.54
	Moisture, pH, NH$_4$-N, SN, CN, sand, clay	7	0.66	0.62	0.54
	Moisture, pH, NH$_4$-N, SN, CN, sand	6	0.66	0.62	0.54
	Moisture, NH$_4$-N, SN, CN, sand	5	0.66	0.63	0.53
	Moisture, SN, CN, sand	4	0.66	0.63	0.53
	Moisture, SN, CN	3	0.63	0.66	0.51
	Moisture, SN	2	0.66	0.63	0.53
	Moisture	2	0.77	0.50	0.64
Combined	Elevation, slope, aspect, TWI, TPI, NDVI, GNDVI, NDMI, temperature, moisture, pH, bulk density, NO$_3$-N, NH$_4$-N, DOC, TDN, SOC, SN, CN, sand, silt, clay	12	0.53	0.77	0.43
	Elevation, aspect, TWI, TPI, NDVI, GNDVI, NDMI, temperature, moisture, pH, bulk density, NO$_3$-N, NH$_4$-N, DOC, TDN, SOC, SN, CN, sand, silt, clay	11	0.53	0.77	0.43
	Elevation, aspect, TWI, NDVI, GNDVI, NDMI, temperature, moisture, pH, bulk density, NO$_3$-N, NH$_4$-N, DOC, TDN, SOC, SN, CN, sand, silt, clay	11	0.53	0.77	0.43
	Elevation, aspect, NDVI, GNDVI, NDMI, temperature, moisture, pH, bulk density, NO$_3$-N, NH$_4$-N, DOC, TDN, SOC, SN, CN, sand, silt, clay	10	0.53	0.77	0.43
	Elevation, aspect, NDVI, GNDVI, NDMI, temperature, moisture, pH, bulk density, NO$_3$-N, NH$_4$-N, DOC, SOC, SN, CN, sand, silt, clay	10	0.53	0.77	0.42
	Elevation, aspect, NDVI, GNDVI, NDMI, temperature, moisture, pH, NO$_3$-N, NH$_4$-N, DOC, SOC, SN, CN, sand, silt, clay	17	0.52	0.77	0.42
	Elevation, aspect, NDVI, GNDVI, NDMI, temperature, moisture, pH, NO$_3$-N, NH$_4$-N, DOC, SOC, SN, CN, sand, clay	16	0.52	0.77	0.42
	Elevation, aspect, NDVI, GNDVI, NDMI, temperature, moisture, pH, NO$_3$-N, NH$_4$-N, DOC, SOC, SN, sand, clay	8	0.52	0.78	0.42
	Elevation, aspect, NDVI, GNDVI, NDMI, temperature, moisture, pH, NO$_3$-N, NH$_4$-N, DOC, SOC, SN, sand	8	0.52	0.78	0.41
	Elevation, aspect, NDVI, GNDVI, NDMI, temperature, moisture, pH, NH$_4$-N, DOC, SOC, SN, sand	7	0.52	0.78	0.41
	Elevation, aspect, NDVI, GNDVI, NDMI, temperature, moisture, pH, NH$_4$-N, SOC, SN, sand	7	0.52	0.78	0.41
	Elevation, aspect, NDVI, GNDVI, NDMI, moisture, pH, NH$_4$-N, SOC, SN, sand	6	0.51	0.78	0.41
	Elevation, aspect, NDVI, GNDVI, NDMI, moisture, pH, SOC, SN, sand	6	0.51	0.78	0.41
	Elevation, aspect, NDVI, GNDVI, NDMI, moisture, SOC, SN, sand	5	0.51	0.78	0.40
	Elevation, aspect, NDVI, GNDVI, NDMI, moisture, SN	5	0.51	0.79	0.40
	Elevation, aspect, NDVI, GNDVI, NDMI, moisture, SN	7	0.51	0.79	0.40
	Elevation, aspect, NDVI, GNDVI, moisture, SN	2	0.49	0.80	0.39
	Elevation, NDVI, GNDVI, moisture, SN	2	0.51	0.79	0.41
	NDVI, GNDVI, moisture, SN	2	0.52	0.78	0.41
	NDVI, GNDVI, moisture	2	0.55	0.75	0.43
	NDVI, GNDVI	2	0.60	0.71	0.47
	GNDVI	2	0.60	0.71	0.49

517

518 **Table B2 a, b, c:** Cross-validation results of different models developed for all (positive and negative) CH₄ fluxes in 2a) forest, 2b)
519 grassland and 2c) arable land using different predictors in the training dataset. Stepwise elimination of least important predictors
520 was implemented.

B2a): Forest CH₄-C (positive & negative) flux		10-fold cross validation			
Category	Predictor variables	mtry	RMSE	R^2	MAE
Remote sensing	Elevation, slope, aspect, TWI, TPI, NDVI, GNDVI, NDMI	2	45.35	0.13	36.00
	Elevation, slope, aspect, TPI, NDVI, GNDVI, NDMI	2	45.26	0.13	35.97
	Elevation, aspect, TPI, NDVI, GNDVI, NDMI	2	45.07	0.15	35.75
	Elevation, aspect, NDVI, GNDVI, NDMI	2	44.63	0.15	35.00
	Aspect, NDVI, GNDVI, NDMI	2	44.79	0.16	35.37
	Aspect, NDVI, GNDVI	2	46.38	0.14	36.15
	Aspect, NDVI	2	47.90	0.12	37.92
	Aspect	2	54.06	0.07	41.44
Site measured soil parameters	Temperature, moisture, pH, bulk density, NO₃-N, NH₄-N, DOC, TDN, SOC, SN, CN, sand, silt, clay	2	44.79	0.16	34.46
	Temperature, moisture, pH, bulk density, NO₃-N, NH₄-N, DOC, SOC, SN, CN, sand, silt, clay	2	44.65	0.16	34.36
	Temperature, moisture, pH, NO₃-N, NH₄-N, DOC, SOC, SN, CN, sand, silt, clay	2	44.52	0.17	34.28
	Temperature, moisture, pH, NO₃-N, NH₄-N, DOC, SOC, SN, CN, sand, silt	2	44.67	0.16	34.36
	Temperature, moisture, pH, NO₃-N, NH₄-N, DOC, SOC, CN, sand, silt	2	44.54	0.16	34.22
	Temperature, moisture, pH, NO₃-N, NH₄-N, DOC, SOC, sand, silt	2	43.98	0.18	33.93
	Temperature, moisture, pH, NO₃-N, DOC, SOC, sand, silt	2	43.64	0.19	33.73
	Temperature, moisture, pH, NO₃-N, DOC, sand, silt	2	43.46	0.19	33.49
	Temperature, moisture, pH, NO₃-N, sand, silt	2	43.07	0.20	33.20
	Temperature, moisture, pH, NO₃-N, silt	2	44.29	0.16	33.87
	Temperature, moisture, pH, NO₃-N	2	45.84	0.14	35.18
	Temperature, moisture, NO₃-N	2	45.31	0.15	35.40
	Moisture, NO₃-N	2	47.94	0.12	36.80
	Moisture	2	51.25	0.08	40.58
Combined	Elevation, slope, aspect, TWI, TPI, NDVI, GNDVI, NDMI, temperature, moisture, pH, bulk density, NO₃-N, NH₄-N, DOC, TDN, SOC, SN, CN, sand, silt, clay	2	44.31	0.17	34.18
	Elevation, slope, aspect, TWI, TPI, NDVI, GNDVI, NDMI, temperature, moisture, pH, bulk density, NO₃-N, NH₄-N, DOC, TDN, SOC, CN, sand, silt, clay	2	44.37	0.17	34.29
	Elevation, aspect, TWI, TPI, NDVI, GNDVI, NDMI, temperature, moisture, pH, bulk density, NO₃-N, NH₄-N, DOC, TDN, SOC, CN, sand, silt, clay	2	44.23	0.18	34.15
	Elevation, aspect, TPI, NDVI, GNDVI, NDMI, temperature, moisture, pH, bulk density, NO₃-N, NH₄-N, DOC, TDN, SOC, CN, sand, silt, clay	2	44.05	0.19	34.05
	Elevation, aspect, NDVI, GNDVI, NDMI, temperature, moisture, pH, bulk density, NO₃-N, NH₄-N, DOC, TDN, SOC, CN, sand, silt, clay	2	43.90	0.19	33.99
	Elevation, aspect, NDVI, GNDVI, NDMI, temperature, moisture, pH, NO₃-N, NH₄-N, DOC, TDN, SOC, CN, sand, silt, clay	2	43.80	0.19	33.88
	Elevation, aspect, NDVI, GNDVI, NDMI, temperature, moisture, pH, NO₃-N, NH₄-N, DOC, SOC, CN, sand, silt, clay	2	43.60	0.20	33.74
	Elevation, aspect, NDVI, GNDVI, NDMI, temperature, moisture, pH, NO₃-N, NH₄-N, DOC, SOC, CN, sand, silt	2	43.64	0.20	33.88
	Elevation, aspect, NDVI, GNDVI, temperature, moisture, pH, NO₃-N, NH₄-N, DOC, SOC, CN, sand, silt	2	43.51	0.20	33.78
	Aspect, NDVI, GNDVI, temperature, moisture, pH, NO₃-N, NH₄-N, DOC, SOC, CN, sand, silt	2	43.48	0.20	33.79
	Aspect, NDVI, GNDVI, temperature, moisture, pH, NO₃-N, DOC, SOC, CN, sand, silt	2	43.03	0.22	33.48
	Aspect, NDVI, GNDVI, temperature, moisture, pH, NO₃-N, DOC, CN, sand, silt	2	42.76	0.22	33.17
	Aspect, NDVI, GNDVI, temperature, moisture, pH, NO₃-N, DOC, CN, silt	2	43.24	0.20	33.49
	Aspect, NDVI, GNDVI, temperature, moisture, pH, NO₃-N, DOC, silt	2	42.81	0.21	33.41
	Aspect, NDVI, GNDVI, temperature, moisture, pH, NO₃-N, silt	2	42.49	0.23	33.30
	Aspect, GNDVI, temperature, moisture, pH, NO₃-N, silt	2	42.71	0.22	33.42
	Aspect, temperature, moisture, pH, NO₃-N, silt	2	43.29	0.20	33.83
	Aspect, temperature, moisture, pH, NO₃-N	2	43.92	0.19	34.69
	Aspect, temperature, moisture, NO₃-N	2	43.50	0.21	34.58
	Temperature, moisture, NO₃-N	2	45.31	0.15	35.40
	Moisture, NO₃-N	2	47.94	0.12	36.80
	Moisture	2	51.25	0.08	40.58

521

B2b): Grassland CH₄-C (positive & negative) flux

Category	Predictor variables	mtry	RMSE	R^2	MAE
Remote sensing	Elevation, slope, aspect, TWI, TPI, NDVI, GNDVI, NDMI	2	28.88	0.15	20.98
	Elevation, slope, aspect, TPI, NDVI, GNDVI, NDMI	2	28.73	0.16	20.97
	Elevation, aspect, TPI, NDVI, GNDVI, NDMI	2	29.19	0.15	21.54
	Elevation, TPI, NDVI, GNDVI, NDMI	2	28.85	0.14	21.56
	Elevation, TPI, NDVI, NDMI	2	29.23	0.15	21.53
	Elevation, TPI, NDMI	2	30.08	0.14	22.04
	Elevation, NDMI	2	30.46	0.13	22.57
	Elevation	2	30.72	0.13	22.84
Site measured soil parameters	Temperature, moisture, pH, bulk density, NO₃-N, NH₄-N, DOC, TDN, SOC, SN, CN, sand, silt, clay	2	26.98	0.22	19.52
	Temperature, moisture, pH, bulk density, NO₃-N, NH₄-N, DOC, TDN, SOC, SN, CN, silt, clay	7	26.96	0.22	19.42
	Temperature, moisture, pH, bulk density, NO₃-N, NH₄-N, DOC, TDN, SN, CN, silt, clay	7	26.86	0.23	19.38
	Temperature, moisture, pH, bulk density, NO₃-N, NH₄-N, DOC, TDN, SN, CN, clay	6	26.66	0.23	19.20
	Temperature, moisture, pH, bulk density, NO₃-N, NH₄-N, DOC, TDN, CN, clay	6	26.68	0.23	19.28
	Temperature, moisture, pH, NO₃-N, NH₄-N, DOC, TDN, CN, clay	5	26.60	0.24	19.16
	Temperature, moisture, pH, NO₃-N, DOC, TDN, CN, clay	2	26.27	0.25	19.00
	Moisture, pH, NO₃-N, DOC, TDN, CN, clay	2	26.16	0.26	19.01
	Moisture, pH, NO₃-N, DOC, CN, clay	2	25.59	0.29	18.62
	Moisture, pH, NO₃-N, DOC, CN	2	26.27	0.25	19.58
	Moisture, pH, DOC, CN	2	26.81	0.23	19.51
	Moisture, DOC, CN	2	26.96	0.24	20.19
	Moisture, CN	2	28.73	0.23	21.43
	Moisture	2	30.95	0.14	23.49
Combined	Elevation, slope, aspect, TWI, TPI, NDVI, GNDVI, NDMI, temperature, moisture, pH, bulk density, NO₃-N, NH₄-N, DOC, TDN, SOC, SN, CN, sand, silt, clay	12	26.91	0.22	19.51
	Elevation, slope, TWI, TPI, NDVI, GNDVI, NDMI, temperature, moisture, pH, bulk density, NO₃-N, NH₄-N, DOC, TDN, SOC, SN, CN, sand, silt, clay	2	26.89	0.22	19.42
	Elevation, slope, TWI, TPI, NDVI, GNDVI, NDMI, temperature, moisture, pH, bulk density, NO₃-N, NH₄-N, DOC, TDN, SOC, SN, CN, sand, clay	2	26.74	0.23	19.36
	Elevation, slope, TWI, TPI, NDVI, GNDVI, NDMI, temperature, moisture, pH, bulk density, NO₃-N, NH₄-N, DOC, TDN, SN, CN, sand, clay	10	26.71	0.23	19.30
	Elevation, slope, TWI, TPI, NDVI, NDMI, temperature, moisture, pH, bulk density, NO₃-N, NH₄-N, DOC, TDN, SN, CN, sand, clay	2	26.56	0.24	19.22
	Elevation, TWI, TPI, NDVI, NDMI, temperature, moisture, pH, bulk density, NO₃-N, NH₄-N, DOC, TDN, SN, CN, sand, clay	2	26.68	0.23	19.39
	Elevation, TPI, NDVI, NDMI, temperature, moisture, pH, bulk density, NO₃-N, NH₄-N, DOC, TDN, SN, CN, sand, clay	2	26.75	0.22	19.36
	Elevation, TPI, NDVI, NDMI, temperature, moisture, pH, bulk density, NO₃-N, NH₄-N, DOC, TDN, SN, CN, clay	2	26.62	0.23	19.29
	Elevation, TPI, NDVI, NDMI, temperature, moisture, pH, bulk density, NO₃-N, NH₄-N, DOC, TDN, CN, clay	2	26.77	0.22	19.35
	Elevation, TPI, NDVI, NDMI, temperature, moisture, pH, NO₃-N, NH₄-N, DOC, TDN, CN, clay	2	26.65	0.23	19.27
	Elevation, TPI, NDVI, NDMI, moisture, pH, NO₃-N, NH₄-N, DOC, TDN, CN, clay	2	26.69	0.22	19.39
	Elevation, TPI, NDVI, NDMI, moisture, pH, NO₃-N, DOC, TDN, CN, clay	2	26.45	0.24	19.29
	Elevation, TPI, NDMI, moisture, pH, NO₃-N, DOC, TDN, CN, clay	2	26.30	0.24	19.14
	TPI, NDMI, moisture, pH, NO₃-N, DOC, TDN, CN, clay	2	26.33	0.25	19.16
	TPI, NDMI, moisture, pH, NO₃-N, DOC, CN, clay	2	25.91	0.27	18.85
	TPI, NDMI, moisture, pH, NO₃-N, CN, clay	2	25.83	0.27	18.62
	TPI, moisture, pH, NO₃-N, CN, clay	2	25.32	0.31	18.18
	Moisture, pH, NO₃-N, CN, clay	2	25.38	0.30	18.29
	Moisture, pH, NO₃-N, CN	2	26.65	0.25	19.61
	Moisture, pH, NO₃-N	2	27.60	0.19	20.52
	Moisture, pH	2	29.67	0.14	22.56
	Moisture	2	30.95	0.14	23.49

522

B2c): Arable CH$_4$-C (positive & negative) flux		**10-fold cross validation**			
Category	**Predictor variables**	**mtry**	**RMSE**	**R^2**	**MAE**
Remote sensing	Elevation, slope, aspect, TWI, TPI, NDVI, GNDVI, NDMI	2	48.58	0.28	33.46
	Elevation, slope, aspect, TWI, NDVI, GNDVI, NDMI	2	48.10	0.28	33.16
	Elevation, slope, aspect, NDVI, GNDVI, NDMI	2	48.79	0.29	33.46
	Elevation, aspect, NDVI, GNDVI, NDMI	2	49.56	0.29	33.54
	Aspect, NDVI, GNDVI, NDMI	2	47.59	0.25	32.46
	Aspect, GNDVI, NDMI	2	48.56	0.26	33.18
	GNDVI, NDMI	2	50.79	0.35	34.72
	NDMI	2	52.71	0.30	36.62
Site measured soil parameters	Temperature, moisture, pH, bulk density, NO$_3$-N, NH$_4$-N, DOC, TDN, SOC, SN, CN, sand, silt, clay	2	45.46	0.24	32.35
	Temperature, moisture, pH, bulk density, NO$_3$-N, NH$_4$-N, DOC, TDN, SOC, SN, CN, silt, clay	2	45.74	0.22	32.67
	Temperature, moisture, pH, bulk density, NO$_3$-N, DOC, TDN, SOC, SN, CN, silt, clay	2	45.73	0.21	32.67
	Temperature, moisture, pH, bulk density, NO$_3$-N, DOC, TDN, SOC, SN, CN, clay	2	45.79	0.21	32.53
	Temperature, moisture, pH, bulk density, NO$_3$-N, DOC, SOC, SN, CN, clay	2	46.74	0.21	33.25
	Temperature, pH, bulk density, NO$_3$-N, DOC, SOC, SN, CN, clay	2	46.81	0.21	33.69
	pH, bulk density, NO$_3$-N, DOC, SOC, SN, CN, clay	2	46.64	0.23	33.38
	pH, bulk density, NO$_3$-N, DOC, SOC, CN, clay	2	45.99	0.23	33.22
	Bulk density, NO$_3$-N, DOC, SOC, CN, clay	2	45.03	0.27	31.97
	Bulk density, NO$_3$-N, DOC, SOC, CN	2	44.43	0.28	32.08
	Bulk density, NO$_3$-N, DOC, CN	2	44.16	0.25	31.82
	NO$_3$-N, DOC, CN	2	43.73	0.30	31.45
	DOC, CN	2	44.51	0.29	32.65
	CN	2	45.77	0.28	34.09
Combined	Elevation, slope, aspect, TWI, TPI, NDVI, GNDVI, NDMI, temperature, moisture, pH, bulk density, NO$_3$-N, NH$_4$-N, DOC, TDN, SOC, SN, CN, sand, silt, clay	2	46.85	0.23	33.13
	Elevation, slope, aspect, TWI, TPI, NDVI, GNDVI, NDMI, temperature, moisture, pH, bulk density, NO$_3$-N, DOC, TDN, SOC, SN, CN, sand, silt, clay	2	46.91	0.21	33.19
	Elevation, slope, aspect, TWI, NDVI, GNDVI, NDMI, temperature, moisture, pH, bulk density, NO$_3$-N, DOC, TDN, SOC, SN, CN, sand, silt, clay	2	46.60	0.22	32.99
	Elevation, slope, aspect, NDVI, GNDVI, NDMI, temperature, moisture, pH, bulk density, NO$_3$-N, DOC, TDN, SOC, SN, CN, sand, silt, clay	2	46.83	0.22	33.03
	Elevation, slope, aspect, NDVI, GNDVI, NDMI, temperature, moisture, pH, bulk density, NO$_3$-N, DOC, TDN, SOC, SN, CN, sand, clay	2	46.87	0.23	33.01
	Elevation, slope, aspect, NDVI, GNDVI, NDMI, temperature, moisture, pH, bulk density, NO$_3$-N, DOC, TDN, SOC, SN, CN, clay	2	47.11	0.25	33.25
	Elevation, aspect, NDVI, GNDVI, NDMI, temperature, moisture, pH, bulk density, NO$_3$-N, DOC, TDN, SOC, SN, CN, clay	2	46.86	0.23	32.89
	Elevation, aspect, NDVI, GNDVI, NDMI, temperature, moisture, pH, bulk density, NO$_3$-N, DOC, SOC, SN, CN, clay	2	47.79	0.26	33.60
	Elevation, aspect, NDVI, GNDVI, NDMI, temperature, moisture, pH, bulk density, NO$_3$-N, DOC, SOC, CN, clay	2	47.86	0.25	33.69
	Elevation, aspect, NDVI, GNDVI, NDMI, moisture, pH, bulk density, NO$_3$-N, DOC, SOC, CN, clay	2	47.62	0.25	33.38
	Elevation, aspect, NDVI, GNDVI, NDMI, pH, bulk density, NO$_3$-N, DOC, SOC, CN, clay	2	47.28	0.24	33.32
	Elevation, aspect, NDVI, GNDVI, NDMI, pH, bulk density, NO$_3$-N, DOC, SOC, CN	2	46.41	0.22	32.75
	Elevation, aspect, NDVI, GNDVI, NDMI, pH, NO$_3$-N, DOC, SOC, CN	2	46.44	0.22	32.65
	Elevation, aspect, NDVI, GNDVI, NDMI, pH, NO$_3$-N, DOC, CN	2	46.67	0.23	32.67
	Elevation, aspect, GNDVI, NDMI, pH, NO$_3$-N, DOC, CN	2	46.47	0.23	32.76
	Elevation, aspect, GNDVI, NDMI, pH, NO$_3$-N, CN	2	47.43	0.25	33.18
	Elevation, aspect, NDMI, pH, CN	2	47.10	0.25	32.74
	Elevation, aspect, GNDVI, NDMI, CN	3	47.49	0.26	32.67
	Aspect, GNDVI, NDMI, CN	2	46.05	0.23	31.87
	GNDVI, NDMI, CN	2	47.59	0.31	33.30
	NDMI, CN	2	47.29	0.24	33.50
	CN	2	45.77	0.28	34.09

523

524 **Table B3 a, b, c:** Cross-validation results of different models developed for all (positive and negative) N₂O fluxes in 3a) forest, 3b)
525 grassland and 3c) arable land using different predictors in the training dataset. Stepwise elimination of least important predictors
526 was implemented.

B3a): Forest N$_2$O-N (positive & negative) flux		10-fold cross validation			
Category	**Predictor variables**	**mtry**	**RMSE**	**R^2**	**MAE**
Remote sensing	Elevation, slope, aspect, TWI, TPI, NDVI, GNDVI, NDMI	2	0.43	0.11	0.30
	Elevation, aspect, TWI, TPI, NDVI, GNDVI, NDMI	2	0.42	0.11	0.30
	Elevation, TPI, NDVI, GNDVI, NDMI	2	0.42	0.11	0.30
	Elevation, aspect, NDVI, GNDVI, NDMI	2	0.43	0.09	0.31
	Aspect, NDVI, GNDVI, NDMI	2	0.44	0.12	0.33
	NDVI, GNDVI, NDMI	2	0.43	0.13	0.32
	NDVI, GNDVI	2	0.45	0.11	0.33
	GNDVI	2	0.46	0.12	0.34
Site measured soil parameters	Temperature, moisture, pH, bulk density, NO$_3$-N, NH$_4$-N, DOC, TDN, SOC, SN, CN, sand, silt, clay	2	0.41	0.12	0.29
	Temperature, moisture, bulk density, NO$_3$-N, NH$_4$-N, DOC, TDN, SOC, SN, CN, sand, silt, clay	2	0.41	0.12	0.29
	Temperature, moisture, bulk density, NO$_3$-N, NH$_4$-N, DOC, TDN, SOC, SN, CN, sand, silt	2	0.41	0.13	0.29
	Temperature, moisture, bulk density, NO$_3$-N, NH$_4$-N, DOC, TDN, SOC, SN, CN, silt	2	0.41	0.14	0.29
	Temperature, moisture, NO$_3$-N, NH$_4$-N, DOC, TDN, SOC, SN, CN, silt	2	0.41	0.13	0.29
	Temperature, moisture, NO$_3$-N, NH$_4$-N, DOC, TDN, SOC, SN, silt	2	0.41	0.12	0.29
	Temperature, moisture, NO$_3$-N, NH$_4$-N, DOC, TDN, SN, silt	2	0.41	0.13	0.29
	Temperature, moisture, NO$_3$-N, NH$_4$-N, TDN, SN, silt	2	0.41	0.15	0.29
	Temperature, moisture, NO$_3$-N, NH$_4$-N, TDN, SN	2	0.41	0.15	0.29
	Temperature, moisture, NO$_3$-N, NH$_4$-N, TDN	2	0.42	0.15	0.30
	Temperature, moisture, NO$_3$-N, NH$_4$-N	2	0.42	0.13	0.30
	Moisture, NO$_3$-N, NH$_4$-N	2	0.42	0.15	0.30
	Moisture, NO$_3$-N	2	0.45	0.11	0.33
	NO$_3$-N	2	0.48	0.11	0.34
Combined	Elevation, slope, aspect, TWI, TPI, NDVI, GNDVI, NDMI, temperature, moisture, pH, bulk density, NO$_3$-N, NH$_4$-N, DOC, TDN, SOC, SN, CN, sand, silt, clay	2	0.41	0.11	0.28
	Elevation, slope, aspect, TWI, TPI, NDVI, GNDVI, NDMI, temperature, moisture, bulk density, NO$_3$-N, NH$_4$-N, DOC, TDN, SOC, SN, CN, sand, silt, clay	2	0.41	0.13	0.28
	Elevation, aspect, TWI, TPI, NDVI, GNDVI, NDMI, temperature, moisture, bulk density, NO$_3$-N, NH$_4$-N, DOC, TDN, SOC, SN, CN, sand, silt, clay	2	0.41	0.12	0.28
	Elevation, aspect, TPI, NDVI, GNDVI, NDMI, temperature, moisture, bulk density, NO$_3$-N, NH$_4$-N, DOC, TDN, SOC, SN, CN, sand, silt, clay	2	0.41	0.12	0.28
	Elevation, aspect, NDVI, GNDVI, NDMI, temperature, moisture, bulk density, NO$_3$-N, NH$_4$-N, DOC, TDN, SOC, SN, CN, sand, silt, clay	2	0.41	0.12	0.29
	Elevation, aspect, NDVI, GNDVI, NDMI, temperature, moisture, bulk density, NO$_3$-N, NH$_4$-N, DOC, TDN, SOC, SN, CN, sand, silt	2	0.41	0.12	0.29
	Elevation, aspect, NDVI, GNDVI, NDMI, temperature, moisture, bulk density, NO$_3$-N, NH$_4$-N, DOC, TDN, SOC, SN, CN, silt	2	0.41	0.13	0.29
	Elevation, aspect, NDVI, GNDVI, NDMI, temperature, moisture, NO$_3$-N, NH$_4$-N, DOC, TDN, SOC, SN, CN, silt	2	0.41	0.12	0.29
	Elevation, aspect, NDVI, GNDVI, temperature, moisture, NO$_3$-N, NH$_4$-N, DOC, TDN, SOC, SN, CN, silt	2	0.41	0.13	0.29
	Elevation, aspect, GNDVI, temperature, moisture, NO$_3$-N, NH$_4$-N, DOC, TDN, SOC, SN, CN, silt	2	0.41	0.13	0.28
	Elevation, aspect, temperature, moisture, NO$_3$-N, NH$_4$-N, DOC, TDN, SOC, SN, CN, silt	2	0.41	0.13	0.28
	Aspect, temperature, moisture, NO$_3$-N, NH$_4$-N, DOC, TDN, SOC, SN, CN, silt	2	0.41	0.13	0.29
	Aspect, temperature, moisture, NO$_3$-N, NH$_4$-N, DOC, TDN, SN, CN, silt	2	0.41	0.13	0.28
	Aspect, temperature, moisture, NO$_3$-N, NH$_4$-N, DOC, TDN, SN, CN	2	0.41	0.14	0.29
	Aspect, temperature, moisture, NO$_3$-N, NH$_4$-N, DOC, TDN, SN	2	0.41	0.15	0.29
	Aspect, temperature, moisture, NO$_3$-N, NH$_4$-N, TDN, SN	2	0.41	0.16	0.29
	Aspect, temperature, moisture, NO$_3$-N, NH$_4$-N, TDN	2	0.42	0.16	0.29
	Temperature, moisture, NO$_3$-N, NH$_4$-N, TDN	2	0.42	0.15	0.30
	Temperature, moisture, NO$_3$-N, NH$_4$-N	2	0.42	0.13	0.30
	Moisture, NO$_3$-N, NH$_4$-N	2	0.42	0.15	0.30
	Moisture, NO$_3$-N	2	0.45	0.11	0.33
	NO$_3$-N	2	0.48	0.11	0.34

527

B3b): Grassland N$_2$O-N (positive & negative) flux

Category	Predictor variables	mtry	RMSE	R^2	MAE
Remote sensing	Elevation, slope, aspect, TWI, TPI, NDVI, GNDVI, NDMI	2	0.73	0.13	0.53
	Elevation, slope, aspect, TPI, NDVI, GNDVI, NDMI	2	0.73	0.13	0.53
	Elevation, aspect, TPI, NDVI, GNDVI, NDMI	2	0.74	0.12	0.55
	Elevation, aspect, NDVI, GNDVI, NDMI	2	0.74	0.14	0.54
	Elevation, NDVI, GNDVI, NDMI	2	0.74	0.14	0.55
	NDVI, GNDVI, NDMI	2	0.76	0.13	0.55
	NDVI, NDMI	2	0.75	0.11	0.57
	NDVI	2	0.78	0.11	0.61
Site measured soil parameters	Temperature, moisture, pH, bulk density, NO$_3$-N, NH$_4$-N, DOC, TDN, SOC, SN, CN, sand, silt, clay	2	0.72	0.12	0.50
	Temperature, moisture, pH, NO$_3$-N, NH$_4$-N, DOC, TDN, SOC, SN, CN, sand, silt, clay	2	0.72	0.12	0.50
	Temperature, moisture, pH, NO$_3$-N, NH$_4$-N, DOC, TDN, SOC, SN, CN, sand, clay	2	0.71	0.15	0.49
	Temperature, moisture, pH, NO$_3$-N, NH$_4$-N, DOC, TDN, SOC, SN, CN, clay	2	0.71	0.15	0.48
	Temperature, moisture, pH, NO$_3$-N, NH$_4$-N, TDN, SOC, SN, CN, clay	2	0.71	0.16	0.49
	Temperature, moisture, pH, NO$_3$-N, NH$_4$-N, SOC, SN, CN, clay	2	0.71	0.15	0.49
	Temperature, moisture, pH, NH$_4$-N, SOC, SN, CN, clay	2	0.71	0.16	0.49
	Temperature, moisture, pH, NH$_4$-N, SOC, CN, clay	2	0.69	0.19	0.48
	Temperature, moisture, NH$_4$-N, SOC, CN, clay	2	0.70	0.19	0.49
	Moisture, NH$_4$-N, SOC, CN, clay	2	0.70	0.18	0.50
	Moisture, NH$_4$-N, CN, clay	2	0.68	0.22	0.49
	Moisture, NH$_4$-N, clay	2	0.70	0.21	0.52
	Moisture, clay	2	0.73	0.22	0.54
	Moisture	2	0.71	0.22	0.53
Combined	Elevation, slope, aspect, TWI, TPI, NDVI, GNDVI, NDMI, temperature, moisture, pH, bulk density, NO$_3$-N, NH$_4$-N, DOC, TDN, SOC, SN, CN, sand, silt, clay	2	0.71	0.14	0.49
	Elevation, slope, aspect, TWI, NDVI, GNDVI, NDMI, temperature, moisture, pH, bulk density, NO$_3$-N, NH$_4$-N, DOC, TDN, SOC, SN, CN, sand, silt, clay	2	0.71	0.16	0.49
	Elevation, aspect, TWI, NDVI, GNDVI, NDMI, temperature, moisture, pH, bulk density, NO$_3$-N, NH$_4$-N, DOC, TDN, SOC, SN, CN, sand, silt, clay	2	0.71	0.16	0.49
	Elevation, aspect, NDVI, GNDVI, NDMI, temperature, moisture, pH, bulk density, NO$_3$-N, NH$_4$-N, DOC, TDN, SOC, SN, CN, sand, silt, clay	2	0.71	0.15	0.49
	Elevation, aspect, NDVI, GNDVI, NDMI, temperature, moisture, pH, NO$_3$-N, NH$_4$-N, DOC, TDN, SOC, SN, CN, sand, silt, clay	2	0.71	0.15	0.49
	Elevation, NDVI, GNDVI, NDMI, temperature, moisture, pH, NO$_3$-N, NH$_4$-N, DOC, TDN, SOC, SN, CN, sand, silt, clay	2	0.71	0.16	0.49
	Elevation, NDVI, GNDVI, NDMI, temperature, moisture, pH, NO$_3$-N, NH$_4$-N, DOC, TDN, SOC, SN, CN, silt, clay	2	0.70	0.17	0.48
	Elevation, NDVI, GNDVI, NDMI, temperature, moisture, pH, NO$_3$-N, NH$_4$-N, DOC, TDN, SOC, SN, CN, clay	2	0.69	0.19	0.47
	NDVI, GNDVI, NDMI, temperature, moisture, pH, NO$_3$-N, NH$_4$-N, DOC, TDN, SOC, SN, CN, clay	2	0.70	0.17	0.48
	NDVI, GNDVI, NDMI, temperature, moisture, pH, NO$_3$-N, NH$_4$-N, TDN, SOC, SN, CN, clay	2	0.70	0.17	0.48
	NDVI, GNDVI, NDMI, temperature, moisture, pH, NH$_4$-N, TDN, SOC, SN, CN, clay	2	0.70	0.18	0.48
	NDVI, GNDVI, NDMI, temperature, moisture, pH, NH$_4$-N, SOC, SN, CN, clay	2	0.70	0.19	0.49
	NDVI, GNDVI, NDMI, temperature, moisture, NH$_4$-N, SOC, SN, CN, clay	2	0.70	0.18	0.49
	NDVI, GNDVI, NDMI, moisture, NH$_4$-N, SOC, SN, CN, clay	2	0.70	0.19	0.48
	NDVI, GNDVI, NDMI, moisture, NH$_4$-N, SOC, CN, clay	2	0.69	0.20	0.48
	NDVI, GNDVI, NDMI, moisture, SOC, CN, clay	2	0.69	0.20	0.48
	NDVI, NDMI, moisture, SOC, CN, clay	2	0.68	0.21	0.48
	NDVI, NDMI, moisture, CN, clay	2	0.68	0.23	0.48
	NDVI, moisture, CN, clay	3	0.67	0.26	0.48
	NDVI, moisture, clay	2	0.71	0.24	0.52
	NDVI, moisture	2	0.67	0.25	0.49
	NDVI	2	0.78	0.11	0.61

528

B3c): Arable N₂O-N (positive & negative) flux — 10-fold cross validation

Category	Predictor variables	mtry	RMSE	R²	MAE
Remote sensing	Elevation, slope, aspect, TWI, TPI, NDVI, GNDVI, NDMI	5	0.49	0.56	0.39
	Elevation, slope, aspect, TWI, NDVI, GNDVI, NDMI	2	0.48	0.58	0.38
	Elevation, aspect, TWI, NDVI, GNDVI, NDMI	2	0.48	0.58	0.37
	Elevation, aspect, NDVI, GNDVI, NDMI	2	0.48	0.58	0.38
	Elevation, NDVI, GNDVI, NDMI	4	0.49	0.57	0.38
	Elevation, GNDVI, NDMI	2	0.49	0.57	0.39
	GNDVI, NDMI	2	0.52	0.53	0.41
	GNDVI	2	0.58	0.45	0.45
Site measured soil parameters	Tmperature, moisture, pH, bulk density, NO₃-N, NH₄-N, DOC, TDN, SOC, SN, CN, sand, silt, clay	8	0.55	0.44	0.44
	Temperature, moisture, pH, NO₃-N, NH₄-N, DOC, TDN, SOC, SN, CN, sand, silt, clay	13	0.54	0.46	0.43
	Temperature, moisture, pH, NO₃-N, NH₄-N, DOC, SOC, SN, CN, sand, silt, clay	12	0.54	0.46	0.43
	Moisture, pH, NO₃-N, NH₄-N, DOC, SOC, SN, CN, sand, silt, clay	11	0.53	0.48	0.42
	Moisture, pH, NO₃-N, NH₄-N, DOC, SOC, SN, CN, sand, silt	10	0.53	0.47	0.43
	Moisture, pH, NO₃-N, DOC, SOC, SN, CN, sand, silt	9	0.53	0.47	0.43
	Moisture, NO₃-N, DOC, SOC, SN, CN, sand, silt	8	0.54	0.46	0.43
	Moisture, NO₃-N, SOC, SN, CN, sand, silt	7	0.54	0.47	0.43
	Moisture, SN, CN, sand, silt	6	0.53	0.48	0.42
	Moisture, NO₃-N, SN, CN, sand	2	0.54	0.47	0.43
	Moisture, NO₃-N, SN, CN	2	0.54	0.46	0.42
	Moisture, SN, CN	2	0.57	0.41	0.45
	Moisture, SN	2	0.58	0.41	0.45
	Moisture	2	0.63	0.33	0.50
Combined	Elevation, slope, aspect, TWI, TPI, NDVI, GNDVI, NDMI, temperature, moisture, pH, bulk density, NO₃-N, NH₄-N, DOC, TDN, SOC, SN, CN, sand, silt, clay	12	0.48	0.57	0.37
	Elevation, aspect, TWI, TPI, NDVI, GNDVI, NDMI, temperature, moisture, pH, bulk density, NO₃-N, NH₄-N, DOC, TDN, SOC, SN, CN, sand, silt, clay	11	0.48	0.57	0.37
	Elevation, aspect, TWI, TPI, NDVI, GNDVI, NDMI, temperature, moisture, pH, bulk density, NO₃-N, NH₄-N, DOC, TDN, SOC, SN, CN, sand, silt	11	0.48	0.57	0.38
	Elevation, aspect, TWI, NDVI, GNDVI, NDMI, temperature, moisture, pH, bulk density, NO₃-N, NH₄-N, DOC, TDN, SOC, SN, CN, sand, silt	10	0.48	0.57	0.37
	Elevation, aspect, NDVI, GNDVI, NDMI, temperature, moisture, pH, bulk density, NO₃-N, NH₄-N, DOC, TDN, SOC, SN, CN, sand, silt	10	0.48	0.57	0.38
	Elevation, aspect, NDVI, GNDVI, NDMI, temperature, moisture, pH, NO₃-N, NH₄-N, DOC, TDN, SOC, SN, CN, sand, silt	9	0.48	0.57	0.38
	Elevation, aspect, NDVI, GNDVI, NDMI, temperature, moisture, pH, NO₃-N, NH₄-N, DOC, TDN, SOC, SN, CN, silt	9	0.48	0.57	0.38
	Elevation, aspect, NDVI, GNDVI, NDMI, temperature, moisture, pH, NO₃-N, NH₄-N, DOC, TDN, SOC, SN, CN	2	0.49	0.57	0.38
	Elevation, NDVI, GNDVI, NDMI, temperature, moisture, pH, NO₃-N, NH₄-N, DOC, TDN, SOC, SN, CN	8	0.48	0.57	0.38
	Elevation, NDVI, GNDVI, NDMI, moisture, pH, NO₃-N, NH₄-N, DOC, TDN, SOC, SN, CN	7	0.48	0.57	0.38
	NDVI, GNDVI, NDMI, moisture, pH, NO₃-N, NH₄-N, DOC, TDN, SOC, SN, CN	7	0.48	0.57	0.38
	NDVI, GNDVI, NDMI, moisture, NO₃-N, NH₄-N, DOC, TDN, SOC, SN, CN	6	0.48	0.57	0.38
	NDVI, GNDVI, NDMI, moisture, NO₃-N, DOC, TDN, SOC, SN, CN	6	0.49	0.56	0.38
	NDVI, GNDVI, NDMI, moisture, NO₃-N, TDN, SOC, SN, CN	2	0.48	0.57	0.38
	NDVI, GNDVI, NDMI, moisture, TDN, SOC, SN, CN	2	0.49	0.56	0.38
	NDVI, GNDVI, NDMI, moisture, TDN, SOC, SN	2	0.49	0.55	0.38
	NDVI, GNDVI, NDMI, moisture, TDN, SN	2	0.48	0.57	0.38
	NDVI, GNDVI, NDMI, moisture, SN	2	0.50	0.54	0.40
	NDVI, GNDVI, NDMI, moisture	2	0.49	0.56	0.39
	GNDVI, NDMI, moisture	2	0.52	0.52	0.41
	GNDVI, NDMI	2	0.52	0.53	0.41
	GNDVI	2	0.58	0.45	0.45

529

Table B4 a, b, c: Cross-validation results of different models developed for negative CH_4 fluxes in 4a) forest, 4b) grassland and 4c) arable land using different predictors in the training dataset. Stepwise elimination of least important predictors was implemented.

Category	Predictor variables	mtry	RMSE	R^2	MAE
B4a): Forest CH_4-C negative fluxes only			**10-fold cross validation**		
Remote sensing	Elevation, slope, aspect, TWI, TPI, NDVI, GNDVI, NDMI	8	39.38	0.21	32.51
	Elevation, slope, aspect, TPI, NDVI, GNDVI, NDMI	2	39.45	0.20	32.64
	Elevation, aspect, TPI, NDVI, GNDVI, NDMI	2	39.11	0.20	32.45
	Elevation, NDVI, GNDVI, NDMI	5	39.53	0.20	32.43
	Elevation, aspect, NDVI, NDMI	4	39.76	0.20	32.57
	Elevation, aspect, NDVI	3	40.42	0.19	32.69
	Aspect, NDVI	2	41.52	0.17	33.61
	Aspect	2	46.08	0.09	35.89
Site measured soil parameters	Temperature, moisture, pH, bulk density, NO$_3$-N, NH$_4$-N, DOC, TDN, SOC, SN, CN, sand, silt, clay	2	40.59	0.14	32.82
	Temperature, moisture, pH, bulk density, NO$_3$-N, NH$_4$-N, DOC, TDN, SOC, SN, sand, silt, clay	2	40.17	0.16	32.57
	Temperature, moisture, pH, NO$_3$-N, NH$_4$-N, DOC, TDN, SOC, SN, sand, silt, clay	2	40.09	0.17	32.52
	Moisture, pH, NO$_3$-N, NH$_4$-N, DOC, TDN, SOC, SN, sand, silt, clay	2	40.16	0.16	32.68
	Moisture, pH, NO$_3$-N, NH$_4$-N, DOC, TDN, SOC, SN, sand, silt	2	40.22	0.16	32.65
	Moisture, pH, NO$_3$-N, NH$_4$-N, DOC, TDN, SOC, SN, sand	5	40.66	0.16	32.59
	Moisture, pH, NO$_3$-N, NH$_4$-N, DOC, SOC, SN, sand	2	40.33	0.16	32.35
	Moisture, pH, NO$_3$-N, DOC, SOC, SN, sand	2	40.02	0.17	32.19
	Moisture, pH, NO$_3$-N, SOC, SN, sand	2	40.21	0.17	32.05
	Moisture, pH, NO$_3$-N, SOC, sand	2	40.01	0.18	31.78
	Moisture, pH, NO$_3$-N, SOC	2	41.27	0.14	32.39
	Moisture, pH, NO$_3$-N	2	41.67	0.15	32.38
	pH, NO$_3$-N	2	43.94	0.12	34.03
	NO$_3$-N	2	47.96	0.10	37.11
Combined	Elevation, slope, aspect, TWI, TPI, NDVI, GNDVI, NDMI, temperature, moisture, pH, bulk density, NO$_3$-N, NH$_4$-N, DOC, TDN, SOC, SN, CN, sand, silt, clay	12	39.66	0.19	32.09
	Elevation, aspect, TWI, TPI, NDVI, GNDVI, NDMI, temperature, moisture, pH, bulk density, NO$_3$-N, NH$_4$-N, DOC, TDN, SOC, SN, CN, sand, silt, clay	11	39.59	0.20	32.09
	Elevation, aspect, TWI, TPI, NDVI, GNDVI, NDMI, temperature, moisture, pH, bulk density, NO$_3$-N, NH$_4$-N, DOC, TDN, SOC, SN, sand, silt, clay	20	39.49	0.20	31.90
	Elevation, aspect, TPI, NDVI, GNDVI, NDMI, temperature, moisture, pH, bulk density, NO$_3$-N, NH$_4$-N, DOC, TDN, SOC, SN, sand, silt, clay	10	39.17	0.21	31.82
	Elevation, aspect, TPI, NDVI, GNDVI, temperature, moisture, pH, bulk density, NO$_3$-N, NH$_4$-N, DOC, TDN, SOC, SN, sand, silt, clay	10	39.11	0.21	31.73
	Elevation, aspect, TPI, NDVI, GNDVI, temperature, moisture, pH, NO$_3$-N, NH$_4$-N, DOC, TDN, SOC, SN, sand, silt, clay	9	38.95	0.22	31.61
	Elevation, aspect, TPI, NDVI, GNDVI, temperature, moisture, pH, NO$_3$-N, NH$_4$-N, DOC, SOC, SN, sand, silt, clay	9	38.79	0.23	31.43
	Elevation, aspect, NDVI, GNDVI, temperature, moisture, pH, NO$_3$-N, NH$_4$-N, DOC, SOC, SN, sand, silt, clay	8	38.73	0.23	31.44
	Elevation, aspect, NDVI, GNDVI, temperature, moisture, pH, NO$_3$-N, DOC, SOC, SN, sand, silt, clay	8	38.48	0.24	31.20
	Elevation, aspect, NDVI, GNDVI, temperature, moisture, pH, NO$_3$-N, DOC, SOC, SN, sand, silt	7	38.35	0.24	31.11
	Elevation, aspect, NDVI, GNDVI, temperature, moisture, pH, NO$_3$-N, SOC, SN, sand, silt	2	37.86	0.26	30.79
	Aspect, NDVI, GNDVI, temperature, moisture, pH, NO$_3$-N, SOC, SN, sand, silt	2	37.55	0.28	30.57
	Aspect, NDVI, GNDVI, temperature, moisture, pH, NO$_3$-N, SOC, SN, silt	2	37.75	0.27	30.72
	Aspect, NDVI, GNDVI, moisture, pH, NO$_3$-N, SOC, SN, silt	2	37.96	0.25	31.07
	Aspect, NDVI, GNDVI, moisture, pH, NO$_3$-N, SOC, SN	2	38.00	0.25	31.04
	Aspect, NDVI, GNDVI, moisture, pH, NO$_3$-N, SOC	2	37.88	0.25	30.83
	Aspect, NDVI, moisture, pH, NO$_3$-N, SOC	2	37.98	0.25	30.87
	Aspect, moisture, pH, NO$_3$-N, SOC	2	38.83	0.22	31.24
	Aspect, moisture, pH, NO$_3$-N	2	38.25	0.25	30.70
	Aspect, pH, NO$_3$-N	2	39.96	0.21	31.88
	Aspect, NO$_3$-N	2	41.25	0.19	32.84
	Aspect	2	46.08	0.09	35.89

Category	Predictor variables	mtry	RMSE	R^2	MAE
B4b): Grassland CH₄-C negative fluxes only		**10-fold cross validation**			
Remote sensing	Elevation, slope, aspect, TWI, TPI, NDVI, GNDVI, NDMI	2	17.33	0.15	13.63
	Elevation, slope, aspect, TPI, NDVI, GNDVI, NDMI	2	17.23	0.15	13.58
	Elevation, aspect, TPI, NDVI, GNDVI, NDMI	2	17.28	0.14	13.70
	Elevation, TPI, NDVI, GNDVI, NDMI	2	16.93	0.17	13.53
	Elevation, NDVI, GNDVI, NDMI	2	17.00	0.16	13.71
	NDVI, GNDVI, NDMI	2	17.14	0.16	13.63
	NDVI, NDMI	2	17.66	0.15	14.11
	NDMI	2	17.72	0.18	13.86
Site measured soil parameters	Temperature, moisture, pH, bulk density, NO₃-N, NH₄-N, DOC, TDN, SOC, SN, CN, sand, silt, clay	2	15.86	0.25	12.37
	Temperature, moisture, pH, bulk density, NO₃-N, DOC, TDN, SOC, SN, CN, sand, silt, clay	2	15.70	0.27	12.21
	Moisture, pH, bulk density, NO₃-N, DOC, TDN, SOC, SN, CN, sand, silt, clay	2	15.50	0.29	12.07
	Moisture, pH, bulk density, NO₃-N, DOC, TDN, SN, CN, sand, silt, clay	2	15.47	0.29	12.04
	Moisture, pH, bulk density, NO₃-N, DOC, SN, CN, sand, silt, clay	2	15.35	0.31	11.95
	Moisture, pH, bulk density, DOC, SN, CN, sand, silt, clay	2	15.39	0.30	12.00
	Moisture, pH, bulk density, DOC, CN, sand, silt, clay	2	15.29	0.31	11.94
	Moisture, pH, DOC, CN, sand, silt, clay	2	15.36	0.30	12.05
	Moisture, pH, DOC, CN, silt, clay	2	15.40	0.30	12.01
	Moisture, pH, CN, silt, clay	2	15.14	0.33	11.79
	Moisture, pH, CN, clay	2	15.32	0.33	11.77
	pH, CN, clay	2	15.61	0.33	11.69
	pH, clay	2	15.80	0.33	11.84
	pH	2	18.06	0.20	14.43
Combined	Elevation, slope, aspect, TWI, TPI, NDVI, GNDVI, NDMI, temperature, moisture, pH, bulk density, NO₃-N, NH₄-N, DOC, TDN, SOC, SN, CN, sand, silt, clay	12	15.70	0.26	12.22
	Elevation, slope, aspect, TWI, TPI, NDVI, GNDVI, NDMI, temperature, moisture, pH, bulk density, NO₃-N, NH₄-N, DOC, TDN, SN, CN, sand, silt, clay	11	15.61	0.27	12.12
	Elevation, slope, aspect, TWI, TPI, NDVI, NDMI, temperature, moisture, pH, bulk density, NO₃-N, NH₄-N, DOC, TDN, SN, CN, sand, silt, clay	11	15.60	0.27	12.12
	Elevation, slope, aspect, TPI, NDVI, NDMI, temperature, moisture, pH, bulk density, NO₃-N, NH₄-N, DOC, TDN, SN, CN, sand, silt, clay	10	15.56	0.28	12.08
	Elevation, slope, aspect, TPI, NDVI, NDMI, temperature, moisture, pH, bulk density, NO₃-N, NH₄-N, DOC, TDN, SN, CN, silt, clay	10	15.52	0.28	12.03
	Elevation, aspect, TPI, NDVI, NDMI, temperature, moisture, pH, bulk density, NO₃-N, NH₄-N, DOC, TDN, SN, CN, silt, clay	9	15.54	0.27	12.10
	Elevation, aspect, TPI, NDVI, NDMI, temperature, moisture, pH, bulk density, NH₄-N, DOC, TDN, SN, CN, silt, clay	9	15.54	0.28	12.07
	Elevation, aspect, TPI, NDVI, NDMI, temperature, moisture, pH, bulk density, DOC, TDN, SN, CN, silt, clay	8	15.37	0.29	11.93
	Elevation, aspect, TPI, NDVI, NDMI, temperature, moisture, pH, bulk density, DOC, TDN, CN, silt, clay	8	15.41	0.29	11.94
	Elevation, TPI, NDVI, NDMI, temperature, moisture, pH, bulk density, DOC, TDN, CN, silt, clay	2	15.16	0.30	11.87
	Elevation, TPI, NDVI, NDMI, moisture, pH, bulk density, DOC, TDN, CN, silt, clay	2	14.98	0.32	11.73
	Elevation, NDVI, NDMI, moisture, pH, bulk density, DOC, TDN, CN, silt, clay	2	15.18	0.29	12.00
	Elevation, NDVI, NDMI, moisture, pH, DOC, TDN, CN, silt, clay	2	15.16	0.29	11.98
	Elevation, NDVI, NDMI, moisture, pH, DOC, CN, silt, clay	2	15.17	0.30	11.98
	Elevation, NDMI, moisture, pH, DOC, CN, silt, clay	2	15.06	0.31	11.76
	NDMI, moisture, pH, DOC, CN, silt, clay	2	15.17	0.31	11.83
	NDMI, moisture, pH, CN, silt, clay	2	14.84	0.34	11.54
	NDMI, moisture, pH, CN, clay	2	14.87	0.34	11.43
	Moisture, pH, CN, clay	2	15.32	0.33	11.77
	pH, CN, clay	2	15.61	0.33	11.69
	pH, clay	2	15.80	0.33	11.84
	pH	2	18.06	0.20	14.43

533

B4c): Arable CH₄-C negatives flux only		10-fold cross validation			
Category	Predictor variables	mtry	RMSE	R^2	MAE
Remote sensing	Elevation, slope, aspect, TWI, TPI, NDVI, GNDVI, NDMI	2	19.54	0.42	14.72
	Elevation, slope, aspect, TWI, NDVI, GNDVI, NDMI	2	19.05	0.44	14.22
	Elevation, slope, aspect, NDVI, GNDVI, NDMI	2	18.72	0.47	13.86
	Elevation, aspect, NDVI, GNDVI, NDMI	2	18.88	0.46	13.89
	Elevation, NDVI, GNDVI, NDMI	2	19.47	0.39	14.92
	Elevation, NDVI, GNDVI	2	19.20	0.40	14.81
	Elevation, GNDVI	2	20.71	0.36	15.66
	GNDVI	2	17.66	0.48	13.16
Site measured soil parameters	Temperature, moisture, pH, bulk density, NO₃-N, NH₄-N, DOC, TDN, SOC, SN, CN, sand, silt, clay	2	17.48	0.50	13.27
	Moisture, pH, bulk density, NO₃-N, NH₄-N, DOC, TDN, SOC, SN, CN, sand, silt, clay	2	17.27	0.52	13.03
	Moisture, pH, bulk density, NO₃-N, NH₄-N, DOC, TDN, SOC, SN, CN, sand, clay	2	17.26	0.52	13.01
	Moisture, pH, bulk density, NO₃-N, NH₄-N, DOC, TDN, SOC, SN, CN, clay	2	17.37	0.52	13.01
	Moisture, pH, bulk density, NH₄-N, DOC, TDN, SOC, SN, CN, clay	2	17.38	0.51	12.96
	Moisture, pH, bulk density, NH₄-N, DOC, SOC, SN, CN, clay	2	17.65	0.50	13.16
	Moisture, pH, NH₄-N, DOC, SOC, SN, CN, clay	2	17.55	0.51	12.92
	Moisture, pH, NH₄-N, DOC, SOC, SN, CN	2	17.67	0.49	13.17
	Moisture, pH, NH₄-N, DOC, SN, CN	2	17.94	0.47	13.27
	Moisture, pH, DOC, SN, CN	2	18.01	0.48	13.29
	Moisture, pH, SN, CN	2	17.77	0.50	13.11
	Moisture, pH, CN	2	17.70	0.50	13.20
	Moisture, CN	2	17.20	0.56	12.84
	CN	2	18.35	0.47	13.70
Combined	Elevation, slope, aspect, TWI, TPI, NDVI, GNDVI, NDMI, temperature, moisture, pH, bulk density, NO₃-N, NH₄-N, DOC, TDN, SOC, SN, CN, sand, silt, clay	22	18.01	0.51	13.33
	Elevation, aspect, TWI, TPI, NDVI, GNDVI, NDMI, temperature, moisture, pH, bulk density, NO₃-N, NH₄-N, DOC, TDN, SOC, SN, CN, sand, silt, clay	21	17.96	0.51	13.26
	Elevation, aspect, TWI, TPI, NDVI, GNDVI, NDMI, temperature, moisture, pH, bulk density, NO₃-N, NH₄-N, DOC, TDN, SOC, SN, CN, sand, clay	20	18.02	0.51	13.29
	Elevation, aspect, TWI, TPI, NDVI, GNDVI, NDMI, moisture, pH, bulk density, NO₃-N, NH₄-N, DOC, TDN, SOC, SN, CN, sand, clay	19	17.92	0.51	13.20
	Elevation, aspect, TPI, NDVI, GNDVI, NDMI, moisture, pH, bulk density, NO₃-N, NH₄-N, DOC, TDN, SOC, SN, CN, sand, clay	18	17.80	0.52	13.14
	Elevation, NDVI, GNDVI, NDMI, moisture, pH, bulk density, NO₃-N, NH₄-N, DOC, TDN, SOC, SN, CN, sand, clay	17	17.77	0.52	13.15
	Elevation, aspect, NDVI, GNDVI, NDMI, moisture, pH, NO₃-N, NH₄-N, DOC, TDN, SOC, SN, CN, sand, clay	2	17.48	0.51	13.04
	Elevation, aspect, NDVI, GNDVI, NDMI, moisture, pH, NO₃-N, NH₄-N, DOC, TDN, SOC, SN, CN, clay	2	17.66	0.51	13.11
	Elevation, aspect, NDVI, GNDVI, NDMI, moisture, pH, NO₃-N, NH₄-N, DOC, TDN, SN, CN, clay	2	17.60	0.51	13.04
	Elevation, aspect, NDVI, GNDVI, NDMI, moisture, pH, NH₄-N, DOC, TDN, SN, CN, clay	2	17.57	0.52	13.04
	Elevation, aspect, NDVI, GNDVI, NDMI, moisture, pH, NH₄-N, DOC, SN, CN, clay	2	17.85	0.50	13.25
	Elevation, aspect, NDVI, GNDVI, NDMI, moisture, pH, DOC, SN, CN, clay	2	17.73	0.51	13.12
	Elevation, aspect, NDVI, GNDVI, NDMI, moisture, pH, DOC, SN, CN	2	17.71	0.51	13.27
	Elevation, NDVI, GNDVI, NDMI, moisture, pH, DOC, SN, CN	2	18.25	0.47	14.02
	Elevation, NDVI, GNDVI, NDMI, moisture, pH, DOC, CN	2	18.26	0.46	14.10
	Elevation, GNDVI, NDMI, moisture, pH, DOC, CN	2	18.45	0.47	14.12
	Elevation, GNDVI, NDMI, moisture, pH, CN	2	18.36	0.47	14.13
	Elevation, GNDVI, moisture, pH, CN	2	18.12	0.48	13.93
	GNDVI, moisture, pH, CN	2	17.79	0.49	13.49
	Moisture, pH, CN	2	17.70	0.50	13.20
	Moisture, CN	2	17.20	0.56	12.84
	CN	2	18.35	0.47	13.70

534

Table B5 a, b, c: Cross-validation results of different models developed for positive N₂O fluxes in 5a) forest, 5b) grassland and 5c) arable land using different predictors in the training dataset. Stepwise elimination of least important predictors was implemented.

B5a): Forest N$_2$O-N positive fluxes only		10-fold cross validation			
Category	Predictor variables	mtry	RMSE	R^2	MAE
Remote sensing	Elevation, slope, aspect, TWI, TPI, NDVI, GNDVI, NDMI	2	0.34	0.15	0.24
	Elevation, aspect, TWI, TPI, NDVI, GNDVI, NDMI	2	0.34	0.15	0.24
	Elevation, aspect, TPI, NDVI, GNDVI, NDMI	2	0.33	0.17	0.23
	Elevation, aspect, NDVI, GNDVI, NDMI	2	0.33	0.19	0.24
	Aspect, NDVI, GNDVI, NDMI	2	0.33	0.23	0.23
	Aspect, NDVI, NDMI	2	0.33	0.19	0.24
	Aspect, NDVI	2	0.33	0.26	0.23
	NDVI	2	0.36	0.19	0.24
Site measured soil parameters	Temperature, moisture, pH, bulk density, NO₃-N, NH₄-N, DOC, TDN, SOC, SN, CN, sand, silt, clay	14	0.31	0.24	0.23
	Temperature, moisture, pH, bulk density, NO₃-N, DOC, TDN, SOC, SN, CN, sand, silt, clay	13	0.31	0.23	0.23
	Temperature, moisture, bulk density, NO₃-N, DOC, TDN, SOC, SN, CN, sand, silt, clay	12	0.31	0.24	0.22
	Temperature, moisture, bulk density, NO₃-N, DOC, TDN, SOC, CN, sand, silt, clay	11	0.31	0.25	0.22
	Temperature, moisture, bulk density, NO₃-N, DOC, TDN, SOC, sand, silt, clay	10	0.31	0.25	0.22
	Temperature, moisture, bulk density, NO₃-N, DOC, TDN, sand, silt, clay	9	0.31	0.25	0.22
	Temperature, moisture, bulk density, NO₃-N, DOC, sand, silt, clay	8	0.31	0.25	0.22
	Temperature, moisture, bulk density, NO₃-N, DOC, silt, clay	7	0.30	0.26	0.22
	Temperature, moisture, bulk density, NO₃-N, silt, clay	6	0.31	0.26	0.22
	Moisture, bulk density, NO₃-N, silt, clay	2	0.31	0.27	0.22
	Moisture, bulk density, silt, clay	2	0.32	0.20	0.23
	Moisture, silt, clay	2	0.33	0.19	0.24
	Silt, clay	2	0.35	0.17	0.25
	Silt	2	0.36	0.16	0.26
Combined	Elevation, slope, aspect, TWI, TPI, NDVI, GNDVI, NDMI, temperature, moisture, pH, bulk density, NO₃-N, NH₄-N, DOC, TDN, SOC, SN, CN, sand, silt, clay	22	0.30	0.25	0.22
	Elevation, slope, aspect, TWI, TPI, GNDVI, NDMI, temperature, moisture, pH, bulk density, NO₃-N, NH₄-N, DOC, TDN, SOC, SN, CN, sand, silt, clay	21	0.30	0.25	0.22
	Elevation, slope, aspect, TPI, GNDVI, NDMI, temperature, moisture, pH, bulk density, NO₃-N, NH₄-N, DOC, TDN, SOC, SN, CN, sand, silt, clay	20	0.30	0.25	0.22
	Elevation, slope, aspect, GNDVI, NDMI, temperature, moisture, pH, bulk density, NO₃-N, NH₄-N, DOC, TDN, SOC, SN, CN, sand, silt, clay	19	0.30	0.25	0.22
	Elevation, aspect, GNDVI, NDMI, temperature, moisture, pH, bulk density, NO₃-N, NH₄-N, DOC, TDN, SOC, SN, CN, sand, silt, clay	18	0.30	0.25	0.22
	Elevation, aspect, GNDVI, NDMI, temperature, moisture, pH, bulk density, NO₃-N, DOC, TDN, SOC, SN, CN, sand, silt, clay	17	0.30	0.25	0.22
	Elevation, aspect, GNDVI, NDMI, temperature, moisture, pH, bulk density, NO₃-N, DOC, TDN, SOC, CN, sand, silt, clay	16	0.30	0.26	0.22
	Aspect, GNDVI, NDMI, temperature, moisture, pH, bulk density, NO₃-N, DOC, TDN, SOC, CN, sand, silt, clay	15	0.30	0.26	0.21
	Aspect, GNDVI, NDMI, temperature, moisture, bulk density, NO₃-N, DOC, TDN, SOC, CN, sand, silt, clay	14	0.30	0.26	0.21
	Aspect, GNDVI, NDMI, temperature, moisture, bulk density, NO₃-N, DOC, TDN, SOC, sand, silt, clay	2	0.30	0.28	0.21
	Aspect, GNDVI, NDMI, temperature, moisture, bulk density, NO₃-N, DOC, TDN, sand, silt, clay	2	0.30	0.28	0.21
	Aspect, NDMI, temperature, moisture, bulk density, NO₃-N, DOC, TDN, sand, silt, clay	2	0.30	0.26	0.22
	Aspect, NDMI, temperature, moisture, bulk density, NO₃-N, DOC, sand, silt, clay	2	0.30	0.25	0.22
	Aspect, temperature, moisture, bulk density, NO₃-N, DOC, sand, silt, clay	5	0.30	0.25	0.22
	Aspect, temperature, moisture, bulk density, NO₃-N, DOC, silt, clay	2	0.30	0.26	0.22
	Aspect, temperature, moisture, bulk density, DOC, silt, clay	7	0.30	0.25	0.22
	Aspect, temperature, moisture, DOC, silt, clay	6	0.29	0.26	0.21
	Aspect, temperature, moisture, DOC, silt	5	0.28	0.29	0.21
	Aspect, temperature, moisture, silt	3	0.29	0.26	0.21
	Aspect, moisture, silt	2	0.30	0.27	0.22
	Moisture, silt	2	0.32	0.22	0.23
	Silt	2	0.36	0.16	0.26

B5b): Grassland N$_2$O-N positive fluxes only		10-fold cross validation			
Category	Predictor variables	mtry	RMSE	R^2	MAE
Remote sensing	Elevation, slope, aspect, TWI, TPI, NDVI, GNDVI, NDMI	2	0.50	0.26	0.38
	Elevation, slope, aspect, TPI, NDVI, GNDVI, NDMI	4	0.51	0.26	0.39
	Elevation, slope, aspect, NDVI, GNDVI, NDMI	4	0.51	0.27	0.38
	Elevation, slope, aspect, NDVI, NDMI	2	0.50	0.27	0.37
	Elevation, aspect, NDVI, NDMI	4	0.51	0.25	0.38
	Elevation, NDVI, NDMI	3	0.50	0.25	0.37
	Elevation, NDMI	2	0.49	0.28	0.37
	Elevation	2	0.49	0.35	0.37
Site measured soil parameters	Temperature, moisture, pH, bulk density, NO$_3$-N, NH$_4$-N, DOC, TDN, SOC, SN, CN, sand, silt, clay	2	0.51	0.18	0.38
	Temperature, moisture, pH, bulk density, NO$_3$-N, NH$_4$-N, TDN, SOC, SN, CN, sand, silt, clay	2	0.51	0.19	0.38
	Temperature, moisture, pH, NO$_3$-N, NH$_4$-N, TDN, SOC, SN, CN, sand, silt, clay	2	0.50	0.19	0.37
	Temperature, moisture, pH, NO$_3$-N, NH$_4$-N, TDN, SOC, SN, CN, silt, clay	2	0.50	0.20	0.37
	Moisture, pH, NO$_3$-N, NH$_4$-N, TDN, SOC, SN, CN, silt, clay	2	0.50	0.19	0.38
	Moisture, pH, NO$_3$-N, NH$_4$-N, TDN, SOC, SN, CN, clay	2	0.50	0.22	0.38
	Moisture, pH, NO$_3$-N, NH$_4$-N, TDN, SN, CN, clay	2	0.50	0.22	0.37
	Moisture, pH, NH$_4$-N, TDN, SN, CN, clay	2	0.50	0.23	0.37
	Moisture, NH$_4$-N, TDN, SN, CN, clay	2	0.49	0.25	0.37
	Moisture, NH$_4$-N, TDN, CN, clay	2	0.49	0.26	0.37
	Moisture, TDN, CN, clay	2	0.47	0.33	0.35
	Moisture, TDN, clay	2	0.45	0.37	0.33
	Moisture, clay	2	0.49	0.31	0.36
	Moisture	2	0.51	0.25	0.35
Combined	Elevation, slope, aspect, TWI, TPI, NDVI, GNDVI, NDMI, temperature, moisture, pH, bulk density, NO$_3$-N, NH$_4$-N, DOC, TDN, SOC, SN, CN, sand, silt, clay	2	0.49	0.21	0.37
	Elevation, slope, aspect, TWI, TPI, NDVI, GNDVI, NDMI, temperature, moisture, pH, bulk density, NO$_3$-N, NH$_4$-N, TDN, SOC, SN, CN, sand, silt, clay	2	0.49	0.22	0.37
	Elevation, slope, aspect, TWI, TPI, NDVI, GNDVI, NDMI, temperature, moisture, pH, NO$_3$-N, NH$_4$-N, TDN, SOC, SN, CN, sand, silt, clay	2	0.49	0.23	0.37
	Elevation, slope, aspect, TPI, NDVI, GNDVI, NDMI, temperature, moisture, pH, NO$_3$-N, NH$_4$-N, TDN, SOC, SN, CN, sand, silt, clay	2	0.49	0.23	0.37
	Elevation, slope, aspect, TPI, NDVI, NDMI, temperature, moisture, pH, NO$_3$-N, NH$_4$-N, TDN, SOC, SN, CN, sand, silt, clay	2	0.49	0.24	0.37
	Elevation, slope, aspect, NDVI, NDMI, temperature, moisture, pH, NO$_3$-N, NH$_4$-N, TDN, SOC, SN, CN, sand, silt, clay	2	0.49	0.23	0.37
	Elevation, aspect, NDVI, NDMI, temperature, moisture, pH, NO$_3$-N, NH$_4$-N, TDN, SOC, SN, CN, sand, silt, clay	2	0.49	0.23	0.37
	Elevation, NDVI, NDMI, temperature, moisture, pH, NO$_3$-N, NH$_4$-N, TDN, SOC, SN, CN, sand, silt, clay	2	0.49	0.21	0.37
	Elevation, NDVI, NDMI, temperature, moisture, pH, NO$_3$-N, NH$_4$-N, TDN, SOC, SN, CN, silt, clay	2	0.49	0.22	0.37
	Elevation, NDVI, NDMI, temperature, moisture, pH, NO$_3$-N, NH$_4$-N, TDN, SOC, CN, silt, clay	2	0.49	0.23	0.36
	Elevation, NDVI, NDMI, temperature, moisture, NO$_3$-N, NH$_4$-N, TDN, SOC, CN, silt, clay	2	0.49	0.24	0.36
	Elevation, NDVI, NDMI, temperature, moisture, NO$_3$-N, NH$_4$-N, TDN, CN, silt, clay	2	0.48	0.24	0.35
	Elevation, NDVI, NDMI, moisture, NO$_3$-N, NH$_4$-N, TDN, CN, silt, clay	2	0.48	0.23	0.36
	Elevation, NDVI, NDMI, moisture, NH$_4$-N, TDN, CN, silt, clay	2	0.48	0.26	0.35
	Elevation, NDVI, NDMI, moisture, TDN, CN, silt, clay	2	0.47	0.28	0.35
	Elevation, NDVI, NDMI, moisture, TDN, CN, clay	2	0.46	0.31	0.34
	NDVI, NDMI, moisture, TDN, CN, clay	2	0.47	0.31	0.34
	NDMI, moisture, TDN, CN, clay	2	0.46	0.33	0.34
	NDMI, moisture, TDN, clay	2	0.45	0.37	0.33
	NDMI, moisture, TDN	2	0.46	0.31	0.33
	NDMI, moisture	2	0.42	0.38	0.31
	NDMI	2	0.58	0.11	0.43

538

B5c): Arable N_2O-N positive fluxes only		10-fold cross validation		
Category	Predictor variables	mtry	RMSE R^2	MAE
Remote sensing	Elevation, slope, aspect, TWI, TPI, NDVI, GNDVI, NDMI	5	0.43 0.63	0.34
	Elevation, aspect, TWI, TPI, NDVI, GNDVI, NDMI	4	0.42 0.64	0.34
	Elevation, aspect, TPI, NDVI, GNDVI, NDMI	4	0.41 0.65	0.33
	Elevation, aspect, NDVI, GNDVI, NDMI	2	0.41 0.66	0.32
	Elevation, NDVI, GNDVI, NDMI	2	0.42 0.65	0.33
	NDVI, GNDVI, NDMI	2	0.42 0.65	0.33
	GNDVI, NDMI	2	0.44 0.63	0.34
	GNDVI	2	0.52 0.51	0.40
Site measured soil parameters	Temperature, moisture, pH, bulk density, NO_3-N, NH_4-N, DOC, TDN, SOC, SN, CN, sand, silt, clay	2	0.55 0.39	0.46
	Temperature, moisture, pH, bulk density, NO_3-N, NH_4-N, DOC, TDN, SOC, SN, CN, silt, clay	2	0.55 0.40	0.45
	Temperature, moisture, pH, NO_3-N, NH_4-N, DOC, TDN, SOC, SN, CN, silt, clay	2	0.54 0.41	0.45
	Temperature, moisture, NO_3-N, NH_4-N, DOC, TDN, SOC, SN, CN, silt, clay	2	0.54 0.42	0.45
	Temperature, moisture, NO_3-N, NH_4-N, DOC, TDN, SOC, SN, CN, clay	2	0.54 0.42	0.44
	Moisture, NO_3-N, NH_4-N, DOC, TDN, SOC, SN, CN, clay	2	0.54 0.41	0.44
	Moisture, NO_3-N, NH_4-N, DOC, TDN, SOC, SN, CN	2	0.55 0.38	0.45
	Moisture, NO_3-N, NH_4-N, TDN, SOC, SN, CN	2	0.56 0.39	0.45
	Moisture, NO_3-N, NH_4-N, SOC, SN, CN	4	0.56 0.37	0.46
	Moisture, NO_3-N, NH_4-N, SN, CN	2	0.56 0.39	0.45
	Moisture, NO_3-N, NH_4-N, SN	2	0.55 0.40	0.45
	Moisture, NO_3-N, SN	2	0.56 0.38	0.46
	Moisture, SN	2	0.58 0.34	0.48
	Moisture	2	0.65 0.29	0.52
Combined	Elevation, slope, aspect, TWI, TPI, NDVI, GNDVI, NDMI, temperature, moisture, pH, bulk density, NO_3-N, NH_4-N, DOC, TDN, SOC, SN, CN, sand, silt, clay	12	0.43 0.62	0.34
	Elevation, slope, aspect, TPI, NDVI, GNDVI, NDMI, temperature, moisture, pH, bulk density, NO_3-N, NH_4-N, DOC, TDN, SOC, SN, CN, sand, silt, clay	11	0.43 0.62	0.34
	Elevation, slope, aspect, TPI, NDVI, GNDVI, NDMI, temperature, moisture, pH, bulk density, NO_3-N, NH_4-N, DOC, TDN, SOC, SN, CN, silt, clay	11	0.43 0.62	0.34
	Elevation, aspect, TPI, NDVI, GNDVI, NDMI, temperature, moisture, pH, bulk density, NO_3-N, NH_4-N, DOC, TDN, SOC, SN, CN, silt, clay	10	0.43 0.62	0.34
	Elevation, aspect, TPI, NDVI, GNDVI, NDMI, temperature, moisture, bulk density, NO_3-N, NH_4-N, DOC, TDN, SOC, SN, CN, silt, clay	10	0.42 0.63	0.33
	Elevation, aspect, TPI, NDVI, GNDVI, NDMI, temperature, moisture, bulk density, NO_3-N, NH_4-N, DOC, TDN, SOC, SN, CN, silt	9	0.43 0.63	0.34
	Elevation, aspect, TPI, NDVI, GNDVI, NDMI, temperature, moisture, bulk density, NO_3-N, NH_4-N, DOC, TDN, SOC, SN, CN	9	0.42 0.63	0.33
	Elevation, aspect, TPI, NDVI, GNDVI, NDMI, temperature, moisture, NO_3-N, NH_4-N, DOC, TDN, SOC, SN, CN	8	0.42 0.64	0.33
	Elevation, aspect, NDVI, GNDVI, NDMI, temperature, moisture, NO_3-N, NH_4-N, DOC, TDN, SOC, SN, CN	8	0.42 0.64	0.33
	Elevation, aspect, NDVI, GNDVI, NDMI, temperature, moisture, NO_3-N, NH_4-N, DOC, TDN, SOC, CN	7	0.41 0.65	0.32
	Elevation, aspect, NDVI, GNDVI, NDMI, temperature, moisture, NO_3-N, DOC, TDN, SOC, CN	7	0.41 0.65	0.33
	Elevation, NDVI, GNDVI, NDMI, temperature, moisture, NO_3-N, DOC, TDN, SOC, CN	6	0.42 0.65	0.33
	Elevation, NDVI, GNDVI, NDMI, temperature, moisture, NO_3-N, TDN, SOC, CN	6	0.41 0.65	0.32
	NDVI, GNDVI, NDMI, temperature, moisture, NO_3-N, TDN, SOC, CN	5	0.41 0.66	0.32
	NDVI, GNDVI, NDMI, moisture, NO_3-N, TDN, SOC, CN	5	0.41 0.66	0.32
	NDVI, GNDVI, NDMI, moisture, NO_3-N, TDN, CN	4	0.40 0.68	0.31
	NDVI, GNDVI, NDMI, moisture, TDN, CN	6	0.40 0.68	0.31
	GNDVI, NDMI, moisture, TDN, CN	5	0.40 0.68	0.31
	GNDVI, NDMI, TDN, CN	3	0.39 0.69	0.31
	GNDVI, NDMI, TDN	3	0.37 0.72	0.30
	GNDVI, NDMI	2	0.44 0.63	0.34
	GNDVI	2	0.52 0.51	0.40

539

540 **Table B6:** The minimum, maximum, mean, standard deviation, and standard error of the measured fluxes at all the sampling points
541 and the predicted landscape fluxes using remote sensing (RS), soil properties (SP), and combined data (CD).

Measured fluxes at sampling points		Summer					Autumn				
Land use	Flux type	Min	Max	Mean	STDEV	SE	Min	Max	Mean	STDEV	SE
Forest		60	589	210	111	12.0	10	446	74	53	5.5
Grassland	SR/ER-CO$_2$-C (mg m^{-2} h^{-1})	136	693	350	123	14.1	9	419	131	82	8.6
Arable		78	877	431	192	23.3	14	238	84	51	6.1
Forest		-201	176	-62	47	5.1	-214	7	-68	48	4.9
Grassland	CH$_4$-C (µg m^{-2} h^{-1})	-84	221	-9	43	5.2	-100	28	-23	21	2.4
Arable		-133	157	8	74	12.3	-43	11	-17	10	1.4
Forest		-13	117	14	24	2.9	-17	78	5	11	1.3
Grassland	N$_2$O-N (µg m^{-2} h^{-1})	-17	281	32	57	7.0	-18	154	12	30	3.7
Arable		13	282	84	65	8.4	-15	54	12	12	1.6
Predicted landscape fluxes (RS data)											
Forest		37	327	171	51	0.03	38	288	74	26	0.01
Grassland	SR/ER-CO$_2$-C (mg m^{-2} h^{-1})	59	484	294	70	0.10	39	477	186	89	0.13
Arable		35	668	324	111	0.08	28	559	102	86	0.06
Forest		-147	65	-70	21	0.01	-148	65	-72	25	0.01
Grassland	CH$_4$-C (µg m^{-2} h^{-1})	-60	50	-15	17	0.02	-64	32	-18	11	0.02
Arable		-60	89	-5	23	0.02	-60	75	-16	11	0.01
Forest		-8	38	7	5	0.003	-6	27	4	4	0.002
Grassland	N$_2$O-N (µg m^{-2} h^{-1})	-8	144	26	34	0.05	-9	69	12	8	0.01
Arable		0	190	60	33	0.02	-1	183	18	17	0.01
Predicted landscape fluxes (SP data)											
Forest		55	343	194	34	0.02	41	214	70	14	0.01
Grassland	SR/ER-CO$_2$-C (mg m^{-2} h^{-1})	72	470	320	38	0.05	52	319	128	44	0.06
Arable		36	733	266	90	0.06	28	733	124	60	0.04
Forest		-123	54	-51	11	0.01	-138	-29	-51	10	0.01
Grassland	CH$_4$-C (µg m^{-2} h^{-1})	-65	37	-8	8	0.01	-65	13	-10	6	0.01
Arable		-87	85	-7	26	0.02	-67	85	-13	17	0.01
Forest		-9	49	9	7	0.00	-9	23	6	4	0.00
Grassland	N$_2$O-N (µg m^{-2} h^{-1})	-6	124	20	8	0.01	-7	54	7	7	0.01
Arable		12	157	45	10	0.01	0	150	19	9	0.01
Predicted landcsape fluxes (CD data)											
Forest		82	325	185	31	0.02	42	195	66	14	0.01
Grassland	SR/ER-CO$_2$-C (mg m^{-2} h^{-1})	155	496	322	47	0.07	52	349	145	61	0.09
Arable		68	694	321	105	0.08	29	568	110	59	0.04
Forest		-125	55	-57	18	0.01	-136	-27	-59	19	0.01
Grassland	CH$_4$-C (µg m^{-2} h^{-1})	-69	36	-6	9	0.01	-69	13	-11	6	0.01
Arable		-72	78	0	24	0.02	-72	53	-17	11	0.01
Forest		-9	49	9	7	0.00	-9	23	6	4	0.00
Grassland	N$_2$O-N (µg m^{-2} h^{-1})	-9	152	25	31	0.05	-8	83	6	7	0.01
Arable		16	168	58	21	0.02	1	128	16	12	0.01

542

543   **Table B7:** Description of the sampling locations within the common hotspot patches of all three GHG fluxes.

Site ID	Land use	Site description and observed soil properties
Q10	Forest	Riparian forest with alder (*Alnus*) trees, higher soil moisture, nitrate, ammonium and DOC concentrations
Q73	Grassland	Riparian grassland with higher soil moisture, ammonium and DOC concentrations
Q80	Grassland	Riparian grassland with Clover (*Trifolium*) and higher soil moisture
C23	Grassland	Higher soil moisture, nitrate, ammonium and DOC concentrations
C79	Grassland	Higher ammonium and DOC concentrations
C45	Grassland	A lot of Clover (*Trifolium*)
C37	Grassland	A lot of Clover (*Trifolium*)
E7	Grassland	A lot of Clover (*Trifolium*)
C3	Arable land	Barley crops
C13	Arable land	Barley crops and the soils had higher nitrate concentrations
Q20	Arable land	Barley crops
C12	Arable land	Barley crops and the soils had higher soil moisture
C56	Arable land	Wheat crops and the soils had higher soil moisture
C97	Arable land	Wheat crops and the soils had higher nitrate concentrations

544

545 **Acknowledgments**

This work was part of the MINCA (MItigation of Nitrogen pollution at CAtchment scale) research project. The authors gratefully acknowledge the German Research Foundation (DFG) for funding the project (HO6420/1-1, KR5265/1-1). KBB additionally received funds via the Pioneer Center for Research in Sustainable Agricultural Futures (Land-CRAFT), DNRF Grant Number P2. Furthermore, Wangari, E. received doctoral funding from the German Academic Exchange Service (DAAD).

546 **Declaration of competing interest**

The authors declare that they have no conflict of interest.

547 **Author contribution**

Conceptualization: KB, LB, GG, TH, RK, DK, EW. Field measurements and laboratory work: EW, RM, TH. Data analysis: EW, RM, KB. Funding acquisition: KB, RK, TH, DK. Writing-original draft preparation: EW, RM, KB. Writing-final draft: EW, KB, RM, LB, RK, TH, DK, GG.

548 **Data availability**

The data will be made freely available via the Zenodo repository after publishing. However, reviewers can request the data anytime during the review process, and the corresponding author will provide it via email.

549   **References**

Adjuik, T. A., & Davis, S., C.: Machine learning approach to simulate soil CO_2 fluxes under cropping systems. Agronomy, 12, 197, https://doi.org/10.3390/ agronomy12010197, 2022.

Arias-Navarro, C., Diaz-Pines, E., Klatt, S., Brandt, P., Rufino, M. C., Butterbach-Bahl, K., & Verchot, L. V.: Spatial variability of soil N_2O and CO_2 fluxes in different topographic positions in a tropical montane forest in Kenya. Journal of Geophysical Research: Biogeosciences, 3 (122), 514–527, https://doi.org/10.1002/2016JG003667, 2017.

Bannari, A., Morin, D., Bonn, F., & Huete, A., R.: A review of vegetation indices. Remote Sensing Reviews, 13 (1-2), 95-120, DOI: 10.1080/02757259509532298, 1995.

Barton L., McLay C. D. A., Schipper L. A., & Smith C. T.: Annual denitrification rates in agricultural and forest soils: a review. Australian Journal of Soil Research, 37 (6), 1073 – 1094, https://doi.org/10.1071/SR99009, 1999.

Berrar, D.: Cross-validation. Encyclopedia of Bioinformatics and Computational Biology, 1, 542-545, DOI: 10.1016/B978-0-12-809633-8.20349-X, 2018.

Breiman, L.: Random Forests. Machine Learning, 45, 5–32, http://dx.doi.org/10.1023/A:1010933404324, 2001.

Butterbach-Bahl, K., & Dannenmann, M.: Denitrification and associated soil N_2O emissions due to agricultural activities in a changing climate. Current Opinion in Environmental Sustainability, 3, (5), 389-395, DOI 10.1016/j.cosust.2011.08.004, 2011.

Butterbach-Bahl, K., Baggs, E. M., Dannenmann, M., Kiese, R., & Zechmeister-Boltenstern, S.: Nitrous oxide emissions from soils: How well do we understand the processes and their controls? Philosophical Transactions of the Royal Society B: Biological Sciences, *368* (1621), 20130122, https://doi.org/10.1098/rstb.2013.0122, 2013.

Butterbach-Bahl, K., Gettel, G., Kiese, R., Fuchs, K., Werner C., Rahimi, J, Barthel, M., & Merbold, L.: Livestock enclosures in drylands of Sub-Saharan Africa are overlooked hotspots of N_2O emissions. Nature Communications, 11, 4644, https://doi.org/10.1038/s41467-020-18359-y, 2022.

Ciarlo, E., Conti, M., Bartoloni, N.: The effect of moisture on nitrous oxide emissions from soil and the $N_2O/(N_2O+N_2)$ ratio under laboratory conditions. Biology and Fertility of Soils, 43, 675–681, https://doi.org/10.1007/s00374-006-0147-9, 2007.

Dutaur, L., & Verchot, L.: A global inventory of the soil CH_4 sink. Global Biogeochemical Cycles, 21 (4), GB4013, https://doi.org/10.1029/2006GB002734, 2007.

Dhakal, S., J.C. Minx, F.L. Toth, A. Abdel-Aziz, M.J. Figueroa Meza, K. Hubacek, I.G.C. Jonckheere, Yong-Gun
Kim, G.F. Nemet, S. Pachauri, X.C. Tan, T. Wiedmann.: Emissions Trends and Drivers, in: IPCC, 2022:
Climate Change 2022: Mitigation of Climate Change. Contribution of Working Group III to the Sixth
Assessment Report of the Intergovernmental Panel on Climate Change [P.R. Shukla, J. Skea, R. Slade, A. Al
Khourdajie, R. van Diemen, D. McCollum, M. Pathak, S. Some, P. Vyas, R. Fradera, M. Belkacemi, A. Hasija,
G. Lisboa, S. Luz, J. Malley, (eds.)]. Cambridge University Press, Cambridge, UK and New York, NY, USA.
doi: 10.1017/9781009157926.004, 2022.

Dorich, C. D., De Rosa, D., Barton, L., Grace, P., Rowlings, D., Migliorati, M. A., et al.: Global Research Alliance
N_2O chamber methodology guidelines: Guidelines for gap-filling missing measurements. Journal of
Environmental Quality, 49 (5),1186-1202, doi: 10.1002/jeq2.20138, 2020.

Gao, B.: NDWI-A Normalized Difference Water Index for Remote Sensing of vegetation liquid water from space.
Remote Sensing of Environment, 58 (3), 257-266, DOI: 10.1016/S0034-4257(96)00067-3, 1196.

Gitelson, A., A., & Merzlyak, M., N.: Remote sensing of chlorophyll concentration in higher plant leaves. Advances
in Space Research, 22 (5), 689-692, https://doi.org/10.1016/S0273-1177(97)01133-2, 1998.

Gradka, R. & Kwinta, A.: A short review of interpolation methods used for terrain modeling. Geomatics, Land
Management and Landscape, 4, 29–47, https://doi.org/10.15576/GLL/2018.4.29, 2018.

Hagedorn, F., & Bellamy, P.: Hot spots and hot moments for greenhouse gas emissions from soils, in Soil Carbon in
Sensitive European Ecosystems: From Science to Land Management, edited by: Jandl, R., Rodeghiero, M., and
Olsson, M., 13–32, Wiley-Blackwell, Chichester, UK. https://doi.org/10.1002/9781119970255.ch2, 2011.

Hamrani, A., Akbarzadeh, A., Madramootoo, C. A.: Machine learning for predicting greenhouse gas emissions from
agricultural soils. Science of The Total Environment, 741, 140338, DOI: 10.1016/j.scitotenv.2020.140338,
2020.

Han, L., Yu, G.-R., Chen, Z., Zhu, X.-J., Zhang, W.-K., Wang, T.-J., et al.: Spatiotemporal pattern of ecosystem
respiration in China estimated by integration of machine learning with ecological understanding. Global
Biogeochemical Cycles, (11), 36, e2022GB007439, https://doi. org/10.1029/2022GB007439, 2022.

Hassan, M. U., Aamer, M., Mahmood, A., Awan, M. I., Barbanti, L., Seleiman, M. F., Bakhsh, G., Alkharabsheh, H.
M., Babur, E., Shao, J., et al.: Management Strategies to Mitigate N_2O Emissions in Agriculture. Life, 12, 439.
https://doi.org/10.3390/life12030439, 2022.

Hensen, A., Skiba, U., & Famulari, D.: Low cost and state of the art methods to measure nitrous oxide emissions.
Environmental Research Letters, 8 (10), 025022, https://doi.org/10.1088/1748-9326/8/2/025022, 2013.

IPCC.: Summary for policymakers. In P. R. Shukla, J. Skea, E. Calvo Buendia, V. Masson-Delmotte, H.-O. Portner, D. C. Roberts, et al. (Eds.), Climate change and land: An IPCC special report on climate change, desertification, land degradation, sustainable land management, food security, and greenhouse gas fluxes in terrestrial ecosystem, 2019.

Jian, J., Steele, M. K., Thomas, R. Q., Day, S. D., & Hodges, S. C.: Constraining estimates of global soil respiration by quantifying sources of variability. Global Change Biology, 24 (9), 4143–4159, https://doi.org/10.1111/gcb.14301, 2018.

Joshi, D. R., Clay, D. E., Clay, S. A., Moriles-Miller, J., Daigh, A. L., Reicks, G., Westhoff, S.: Quantification and Machine learning based N_2O-N and CO_2-C emissions predictions from a decomposing rye cover crop. Agronomy Journal, https://doi.org/10.1002/agj2.21185, 2022.

Kaiser, K. E., McGlynn, B. L., & Dore, J. E.: Landscape analysis of soil methane flux across complex terrain. Biogeosciences, 15, 3143–3167, https://doi.org/10.5194/bg-15-3143-2018, 2018.

Kuhn, M.: Building Predictive Models in R Using the caret Package. Journal of Statistical Software, 28, (5), 1-26, DOI: 10.18637/jss.v028.i05, 2008.

Le Mer, J., & Roger, P. A.: Production, oxidation, emission and consumption of methane by soils: A review. European Journal of Soil Biology, 1(37), 25–50, https://doi.org/10.1016/S1164-5563(01)01067-6, 2001.

Levy, P., Clement, R., Cowan, N., Keane, B., Myrgiotis, V., van Oijen, M., et al.: Challenges in scaling up greenhouse gas fluxes: Experience from the UK greenhouse gas emissions and feedbacks program. Journal of Geophysical Research: Biogeosciences, 127, e2021JG006743, https://doi.org/10.1029/2021JG006743, 2022.

Malakhov, D. V., & Tsychuyeva, Y. T.: Calculation of the biophysical parameters of vegetation in an arid area of south-eastern Kazakhstan using the normalized difference moisture index (NDMI). Cent. Asian J. Environ. Sci. Technol. Innov., 1 (4), 189-198, DOI: 10.22034/CAJESTI.2020.04.01, 2020.

Malique, F., Ke, P., Boettcher, J., Dannenmann, M., & Butterbach-Bahl, K.: Plant and soil effects on denitrification potential in agricultural soils. Plant Soil, 439 (1–2), 459–474, https://doi.org/10.1007/s11104-019-04038-5, 2019.

Mason, C. W., Stoof, C. R., Richards, B. R, Das, S., & Goodale, C. L.: Hotspots of Nitrous Oxide Emission in Fertilized and Unfertilized Perennial Grasses. Soil Science Society of American Journal, 81, (3), 450-458, DOI: 10.2136/sssaj2016.08.0249, 2017.

McDaniel, M. D., Simpson, R. G., Malone, B. P., McBratney, A. B., Minasny, B., & Adams, M. A.: Quantifying and predicting spatio-temporal variability of soil CH_4 and N_2O fluxes from a seemingly homogeneous Australian agricultural field. Agriculture, Ecosystems and Environment, 240, 182-193, http://dx.doi.org/10.1016/j.agee.2017.02.017, 2017.

Molodovskaya, M., Warland, J., Richards, B. K., Öberg, G., & Steenhuis, T. S.: Nitrous oxide from heterogeneous agricultural landscapes: Source contribution analysis by eddy covariance and chambers. Soil Science Society of American Journal, 75, (5), 1829-1838, https://doi.org/10.2136/sssaj2010.0415, 2011.

Oertel, C., Matschullat, J., Zurba, K., Zimmermann, F., & Erasmi, S.: Greenhouse gas emissions from soils - a review. Geochemistry, 763 (3), 327–352, https://doi.org/10.1016/j.chemer.2016.04.002, 2016.

Philibert, A., Loyce, C., & Makowski, D.: Prediction of N_2O emission from local information with Random Forest. Environmental Pollution, 177, 156-63, doi: 10.1016/j.envpol.2013.02.019, 2013.

Räsänen, A., Manninen, T., Korkiakoski, M., Lohila, A., & Virtanen, T.: Predicting catchment-scale methane fluxes with multi-source remote sensing. Landscape Ecology, 36, 1177–1195, https://doi.org/10.1007/s10980-021-01194-x, 2021.

Rosenstock, T. S., Mariana, C. R., Chirinda, N., van Bussel, L., Reidsma, P., & Butterbach-Bahl, K.: Scaling point and plot measurements of greenhouse gas fluxes, balances, and intensities to whole farms and landscapes. In: Rosenstock, T. S., Mariana, C. R., Butterbach-Bahl, K. Wollenberg, L., & Richards, M. (Eds). 2016. Methods for Measuring Greenhouse Gas Balances and Evaluating Mitigation Options in Smallholder Agriculture. Springer, Switzerland. pp.175-188, 2016.

Saha, D., Basso, B., & Robertson, G. P.: Machine learning improves predictions of agricultural nitrous oxide (N_2O) emissions from intensively managed cropping systems. Environmental Research Letters, 16, (2), 024004, https://doi.org/10.1088/1748-9326/abd2f3, 2021.

Sahraei, A., Kraft, P., Windhorst, D., & Breuer, L.: High-Resolution, in situ monitoring of stable isotopes of water revealed insight into hydrological response behavior. Water, 12 (2), 565, https://doi.org/10.3390/w12020565, 2020.

Sahraei, A., Houska, T., & Breuer, L.: Deep learning for isotope hydrology: The application of long short-term memory to estimate high temporal resolution of the stable isotope concentrations in stream and groundwater. Frontiers in Water, 3, 113, https://doi.org/10.3389/frwa.2021.740044, 2021.

Steinkamp, R., Butterbach-Bahl, K., & Papen, H.: Methane oxidation by soils of an N-limited and N-fertilized spruce forest in the Black Forest, Germany. Soil Biology and Biochemistry, 33(2), 145–153, https://doi.org/10.1016/S0038-0717(00)00124-3, 2000.

Sundqvist, E., Persson, A., Kljun, N., Vestin, P., Chasmer, L., Hopkinson, C., & Lindroth, A.: Upscaling of methane exchange in a boreal forest using soil chamber measurements and high-resolution LiDAR elevation data. Agricultural and Forest Meteorology, 15(214– 215), 393–401, https://doi.org/10.1016/j.agrformet.2015.09.003, 2015.

Tian, H., Xu, R., Canadell, J. G., Thompson, R. L., Winiwarter, W., Suntharalingam, P., et al.: A comprehensive quantification of global nitrous oxide sources and sinks. Nature, 586(7828), 248–256, https://doi.org/10.1038/s41586-020-2780-0, 2020.

Tubiello, F. N., Salvatore, M., Rossi, S., Ferrara, A., Fitton, N., & Smith, P.: The FAOSTAT database of greenhouse gas emissions from agriculture. Environmental Research Letters, 8 (1), [015009], https://doi.org/10.1088/1748-9326/8/1/015009, 2013.

Vainio, E., Peltola, O., Kasurinen, V., Kieloaho, A, Tuittila, E, Pihlatie, M.: Topography-based statistical modelling reveals high spatial variability and seasonal emission patches in forest floor methane flux. Biogeosciences, 18 (6), 2003–2025, https://doi.org/10.5194/bg-18-2003-2021, 2021.

van Kessel, C., Pennock, D. & Farrell, R.: Seasonal variations in denitrification and nitrous oxide evolution at the landscape scale. Soil Sci. Soc. Am. J. 57, 988–995, doi:10.2136/sssaj1993.03615995005700040018x, 1993.

Wagner-Riddle, C., Baggs, E. M., Clough, T. J., Fuchs, K., & Petersen, S. O.: Mitigation of nitrous oxide emissions in the context of nitrogen loss reduction from agroecosystems: managing hot spots and hot moments. Current Opinion in Environmental Sustainability, (47), 46-53, https://doi.org/10.1016/j.cosust.2020.08.002, 2020.

Wangari, E. G., Mwanake, R. M., Kraus, D., Werner, C., Gettel, G. M., Kiese, R., Breuer, L., Butterbach-Bahl, K., & Houska, T.: Number of Chamber Measurement Locations for Accurate Quantification of Landscape-Scale Greenhouse Gas Fluxes: Importance of Land Use, Seasonality, and Greenhouse Gas Type. Journal of Geophysical Research: Biogeosciences, 127 (9), e2022JG006901, https://doi.org/10.1029/2022JG006901, 2022.

Warner, D. L., Guevara, M., Inamdar, S., & Vargas, R.: Upscaling soil-atmosphere CO_2 and CH_4 fluxes across a topographically complex forested landscape. Agricultural and Forest Meteorology, 264, 80–91, https://doi.org/10.1016/j.agrformet.2018.09.020, 2019.

Webster, K. L., Creed, F., Beall, F. D., & Bourbonnie`re, R. A.: Sensitivity of catchment-aggregated estimates of soil carbon dioxide efflux to topography under different climatic conditions. Journal of geophysical research, 113, G03040, doi:10.1029/2008JG000707, 2018.

Zhang, C., Comas, X., & Brodylo, D.: A remote sensing technique to upscale methane emission flux in a subtropical peatland. Journal of Geophysical Research: Biogeosciences, 125, e2020JG006002, https://doi.org/10.1029/2020JG00600, 2020.

550

Plain text summary

Agricultural landscapes act as sinks or sources of the greenhouse gases (GHG) CO2, CH4 or N2O. Fluxes of these
GHGs between ecosystems and the atmosphere are controlled by various physico-chemical and biological
processes. Therefore, fluxes depend on environmental conditions such as moisture, temperature, or soil
parameters, which results in large spatial and temporal variations of GHG fluxes. Here we describe an example
how this variation may be studied and analysed.